OBSERVATION-BASED METHODS (OBMS) FOR ANALYZING URBAN/REGIONAL OZONE PRODUCTION AND OZONE-NO_x-VOC SENSITIVITY.

Dr. Sanford Sillman
Research Scientist
University of Michigan
sillman@umich.edu
http://www-personal.engin.umich.edu/~sillman

Acknowledgement: This site was prepared in conjunction with research supported by the U.S. Environmental Protection Agency under the Science To Improve Results (STAR) program (grant #R826765) and by the EPA Office of Research and Development (grant #F005300). Although the site was prepared with the aid of funding from EPA, it has not been subjected to peer and administrative review by either agency, and therefore may not necessarily reflect the views of the agency, and no official endorsement should be inferred.

Observation-based methods (OBMs) refer to attempts to evaluate the sources of **atmospheric ozone** in urban and polluted rural environments based on inferences made directly from measurements. They are also closely related to the question of how ozone is related to its two main precursors: **nitrogen oxides (NO_x)** and **volatile organic compounds (VOC)**.

This site is intended to provide a guide for researchers and policymakers who would like to use OBMs as part of their evaluation of the sources of ozone. The methods and results shown here are the authors' recommendations only and do not have official support from the U.S. EPA or any other agency.

Complete results: A **draft report to EPA** is available at Dr. Sillman's web site: http://www-personal.engin.umich.edu/~sillman.

Also available: a report on observation-based methods for analyzing ozone-NO_x-VOC sensitivity; and Dr. Sillman's published journal articles. (Go to http://www-personal.engin.umich.edu/~sillman).

CONTENTS:

==========

1. OBSERVATION-BASED METHODS (OBMS): OVERVIEW.

The following gives a concise summary of each of the methods included here. It also introduces the **detailed presentation** for each OBM (Section 2) and the contents of each.

1.1. Goals of OBMs.

The primary purpose of OBMs is to reduce the uncertainty in predictions for the ***impact of reduced NO_x and VOC on O_3*** by using ambient measurements. O_3-NO_x-VOC sensitivity is a major source of uncertainty in ozone-precursor predictions (see **Figure 1.3** in the overview article on ozone NO_x-VOC sensitivity).

A second purpose is to ***evaluate the accuracy of chemistry/transport models***, which seek to represent the process of ozone formation and transport and often provide the basis for predicting the impact of emissions on O_3.

A third purpose is to ***evaluate the accuracy of emission inventories***, which often represent the major uncertainty in chemistry/transport models.

They also provide information about the ***ozone production efficiency (OPE)*** per NO_x, which represents the ratio of ozone production to NO_x removal.

OBMs often provide methods to infer whether ambient O3 is NO_x-sensitive or VOC-sensitive based on ambient measurements. These may include simple ***rules-of-thumb*** that identify conditions as NO_x-sensitive or VOC-sensitive based on the value of certain measured indices. Here, caution is recommended in the use of simple rules of thumb. It is more reliable if the OBM can be expanded to include a ***broad analysis of measured data sets***, which would evaluate the accuracy and applicability of rules of thumb and would identify errors in measurements. This analysis represents essential ***quality assurance*** for the OBM.

The following gives an **overview of individual methods**. Each method is linked to a **detailed presentation**.

1.2. Secondary species as NOx-VOC indicators.

This approach uses measured secondary species – primarily ***reactive nitrogen and peroxides*** – to derive information about O_3-NO_x-VOC sensitivity. The sum of total reactive nitrogen (NO_y, including primary NO_x) is also used.

The secondary species have little direct impact on the ozone formation process. They are usually produced simultaneously with ozone and thus provide information about the conditions under which ozone was formed.

NO_x-VOC indicators are based on results from chemistry/transport models. The model results predict that certain values of NO_x-VOC indicators are associated with NO_x-sensitive conditions, while other values are associated with VOC-sensitive conditions. Some confirmation is provided by results from ambient measurements, which are consistent with predictions associated with indicators.

Initially, the indicator approach was presented as a series of rules-of-thumb that would identify whether O_x was NO_x-sensitive or VOC-sensitive based on ambient measurements. Ratios such as O_3/NO_y, O_3/NO_z (where NO_z represents summed NO_x reaction products, or NO_y-NO_x), and $O3/HNO_3$and $H2O2/HNO_3$ were identified as indicators for NO_x-sensitive chemistry if they exceeded a certain threshold or transition value, and as indicators for VOC-sensitive chemistry if they fell below that value (Sillman, 1995). Subsequent results suggested that the behavior of indicator ratios may be different in different locations (Lu and Chang, 1998).

An expanded version of the indicator concept uses measured patterns of correlation between secondary species (e.g. O_3 vs. NOz, etc.) to make inferences about NO_x-VOC sensitivity and to evaluate chemistry/transport models. This approach is advantageous because the measured correlation patterns can be used to identify erroneous measurements or to identify inconsistencies that would prevent the use of indicator ratios to infer NO_x-VOC sensitivity.

The measured correlation patterns provide a method for evaluating chemistry/transport models. Because the indicator correlations are related to NO_x-VOC sensitivity in models, they provide an test for the accuracy of model NO_x-VOC sensitivity predictions.

The ***detailed presentation*** below (**Section 2)** provides the following.

- The "rules of thumb" for indicator ratios.
- Indicator correlation patterns for NO_x-sensitive and VOC-sensitive locations, from chemistry/transport models and from measurements.
- Use of indicator correlations to evaluate chemistry/transport models.
- Guidelines for practical implementation.

1.3. Smog production algorithms (extent of reaction parameters).

Smog production algorithms represent an attempt to identify NO_x-sensitive and VOC-sensitive conditions based on ambient measurements of O_3, NO_x and/or NO_y.

The algorithms consist of "rules of thumb" for NO_x-sensitive versus VOC-sensitive conditions, derived based on the results of smog chamber experiments.

The "extent-of-reaction" concept posits that NO_x-sensitive conditions are found when photochemistry has been run to completion and most of the emitted NO_x has been removed, while VOC-sensitive conditions are found when the ozone production process has not yet run to completion.

Smog production algorithms have been widely used by EPA and by state governments to evaluate ozone-precursor relationships. They are **not** recommended here. As presented here, the smog production algorithms contain fundamental flaws that should preclude their use. The ***detailed presentation*** below **(Section 3)** identifies these flaws.

For a more positive view of smog production algorithms, refer to Blanchard et al. (1999, 2000) and Blanchard and Stockenius (2001). A more comprehensive description is included in the ***draft report to EPA***.

1.3. Methods based on ambient NO_x and VOC.

NO_x and VOC are direct precursors of ozone formation, and are directly related to O_3-NO_x-VOC sensitivity.

Ambient NO_x and VOC are related to the instantaneous rate of ozone production. It is more difficult to relate ambient NO_x and VOC to ambient O_3, because transport and upwind production must be accounted for.

It is possible to calculate the instantaneous rate of ozone production and its sensitivity to NO_x and VOC, using a 0-d model and measured NO_x and VOC. Kleinman et al. (1997, 2000, 2001) and Tonnessen and Dennis (2000) have also developed simplified formulas for instantaneous NO_x-VOC sensitivity, based on ambient NO_x and reactivity-weighted VOC.

Cardelino et al. (1995, 2000) built a model to calculate overall NO_x-VOC sensitivity in an urban area, based on calculated rates of ozone production at measurement sites throughout the area, driven by measured ambient NO_x and VOC.

Analysis based on ambient NO_x and VOC form a natural complement to the analysis based on secondary species as NOx-VOC indicators.

Methods for calculating ozone production rates and NO_x-VOC sensitivity should be combined with a broader evaluation of measurements, including measured correlations between individual VOC and between VOC and NO_x, inferred emission rates in comparison with inventories, and quality assurance. These methods are described in the next section (1d).

The detailed ***presentation*** **(Section 4)** includes a combined description of methods for deriving NO_x-VOC sensitivity from ambient NO_x and VOC, methods for deriving emission rates, and the recommended broader analysis of measurements.

1.4. Evaluation of emission inventories.

Emission inventories represent the single largest uncertainty in chemistry/transport models for ozone.

Emission inventories can be evaluated using data sets of measured ambient NO_x (or NO_y) and speciated VOC. Parrish et al. (1998, 2001) have described methods for inferring emission rates based on correlations between individual VOC and between VOC and NO_x. These methods also include tests for internal consistency of measurements.

The measured VOC-VOC and VOC-NO_x correlations and/or directly inferred emission rates can be used to evaluate the accuracy of chemistry/transport model applications, and to modify emission rates in these models to insure better agreement with ambient measurements.

Mendoza-Dominguez and Russell (2001a, 2001b) have used measured NO_x and VOC in combination with chemistry/transport models to modify emission inventories, using techniques of inverse modeling.

Evaluation of ambient NO_x and VOC and consistency tests can be combined with analysis of NO_x-VOC sensitivity based on ambient NO_x and VOC.

The ***detailed presentation*** for ambient NOx and VOC **(Section 4)** includes the following:

- Methods for inferring NO_x-VOC sensitivity from ambient NO_x and VOC.
- Methods for inferring emission rates from ambient NO_x and VOC.
- Tests for consistency of the data set for NO_x and VOC.
- Suggestions for practical implementation.

==========

2. SECONDARY SPECIES AS NO_X-VOC INDICATORS.

CONTENTS:

==========

2.1. Why it works: relation between secondary species and O_3-NO_x-VOC sensitivity.

NO_x-VOC indicators mainly involve secondary species that are produced concurrently with photochemical production of O_3. These species are all relatively long-lived and are transported along with O_3. Ratios among these species carry information about the chemistry associated with ozone formation.

Peroxides and nitric acid (HNO_3) are directly related to the chemistry that causes the split into NO_x-sensitive and VOC-sensitive regimes. Under NO_x-sensitive conditions the rate of production of peroxides exceeds the rate of production for HNO_3. Under NO_x-saturated (VOC-sensitive) conditions the rate of production of HNO_3 exceeds the rate of production of peroxides. These production rates are determined by the chemistry of odd hydrogen radicals (OH, HO_2, CH_3O_2, etc.), which also determine O_3-NO_x-VOC sensitivity. (A detailed description of the chemistry of O_3, NO_x and VOC is available at http://www-personal.engin.umich.edu/~sillman).

The ambient ratio of peroxides to HNO_3 reflects the rates of production of these species, except during conditions with rapid removal of these species (rainfall, or dry deposition from a shallow surface layer at night).

Ozone and NO_x reaction products (NO_z) are also related to the NO_x-VOC chemistry, although the relation is less direct.

The ratio of rate of production of O_3 to the rate of production of nitric acid ($p(O_3)/p(HNO_3)$) is closely associated with the ratio of reactivity-weighted VOC to NO_x. This is because production of O_3 is initiated by the reaction of VOC with OH, while the production of HNO_3 occurs through the reaction of NO_2 with OH. The ratio ($p(O_3)/p(HNO_3)$) is also related to the chemistry of odd hydrogen radicals which determines the split into NO_x-sensitive and VOC-sensitive regimes.

The ratio of production of O_3 to removal of NO_x (through chemical conversion to HNO_3 and organic nitrates) is also related to the **ozone production efficiency per NO_x (OPE)**, which is often used in analyses of ozone production chemistry (e.g. Liu et al., 1987, Lin et al., 1988, Trainer et al., 1993).

The slope of ambient O_3 versus summed NO_x reaction products (NO_z) is not exactly equal to the ozone production efficiency, because the slope is also affected by processes that remove NO_x reaction products from the atmosphere (Sillman et al., 1998). However, variations in the slope of O_3 versus NO_z and O_3 versus HNO_3 reflect variations in both ozone production efficiency and O_3-NO_x-VOC sensitivity.

The ratio between **ozone and organic nitrates** is completely unrelated to O_3-NO_x-VOC sensitivity. The ratio of ozone to NO_z carries information about O_3-NO_x-VOC sensitivity only because HNO_3 is a major component of NO_z.

Ozone and total reactive nitrogen (NO_y): The ratio and correlation between O_3 and NO_y reflects two separate processes, both of which are related to O_3-NO_x-VOC sensitivity. It reflects the process of photochemical production of O_3, represented by the ratio between O_3 and NO_z. It also reflects the process of **NO_x titration**, which refers to the immediate removal of O_3 through reaction with directly emitted NO. The other secondary species are unaffected by NO_x titration. A low value for O_3/NO_3 identifies NO_3 saturated chemistry either in the past history of the air mass (reflected by O_3 versus NO_z) or in current conditions (reflected by O_3 versus NO_x).

==========

2.2. Rules of thumb.

The relation between O_3-NO_x-VOC sensitivity and NO_x-VOC indicators was derived from chemistry-transport models. It was found that when models predict VOC-sensitive conditions, they also predict low values for certain ambient indicator ratios. When models predict NO_x-sensitive conditions, they predict high values for the ratios. The same relation between predicted NO_x-VOC sensitivity and indicator ratios appeared in models for several urban areas and regions in the U.S. and in Europe (Sillman, 1995; Sillman et al., 1997, 1998, 2002; Sillman and He, 2002; Tonnessen et al., 2000b; Martilli et al., 2002).

The indicator ratios identified in the above references are: O_3/NO_y, O_3/NO_z, O_3/HNO_3, H_2O_2/HNO_2, total peroxides/HNO_3, and equivalent ratios of peroxides to NO_z and NO_x. Ratios were also identified that used background values of ozone (O_3b) and other species: $(O_3\text{-}O_3b)/(NO_y\text{-}NO_yb)$, $(O_3\text{-}O_3b)/(NO_z\text{-}NO_zb)$, and $(O_3\text{-}O_3b)/(HNO_3\text{-}HNO_3b)$. This is based on a specific definition of ***background ozone***, given below. These ratios refer to values between the hours of **noon and sunset** only, and are related to O_3-NO_x-VOC sensitivity only at the same time and location as the ambient ratio.

Figure 2.1 shows the relation between NO_x-VOC sensitivity in models. The figure shows the predicted reduction in O_3 resulting from either a 35% reduction in emissions of anthropogenic VOC or a 35% reduction in NO_x, for models for several regions in the U.S. (listed in **Table 2.1**). Each point in the figure represents a different model location. All are for afternoon hours, usually close to the time of maximum O_3. The split between NO_x-sensitive and VOC-sensitive locations is clearly visible in the figures. It can be seen that the primarily NO_x-sensitive model locations also have high values for indicator ratios, and VOC-sensitive locations have low values for indicator ratios.

Indicator values for NO_x-sensitive and VOC-sensitive conditions are summarized in **Table 2.2**. Measured values lower than the NO_x-VOC "transition" in the table are generally VOC-sensitive. Measured values higher than the NO_x-VOC transition are generally VOC-sensitive. The median values identify typical indicator ratios for strongly NO_x-sensitive and strongly VOC-sensitive conditions.

Definition: Background values for O_3 and other species are defined as the ambient mixing ratios at a relatively unpolluted upwind site, as measured (or modeled) at as close as possible to the same time as the other ambient values (O_3, NO_y, etc.) of the indicator ratio. This nonstandard definition is used because with this definition it is easy to determine background values from a network of ambient measurements. Model results for indicator ratios were derived based on the same definition. Background values are based on measurements (or model values) at the same time as the other mixing ratios (typically during the afternoon hours) in order to include the impact of entrainment from aloft as the convective mixed layer grows. Given a network of measurements, background values should be selected based on the site with the lowest NO_y for the hour of interest.

WARNING: Somewhat contrary results have been reported by Lu and Chang (1998), Chang et al. (1999) and Blanchard and Stockenius (2000).

It is more accurate to include an examination of measured correlations between secondary species rather than simple rules of thumb. Measured correlation patterns can be compared with predicted correlation patterns from models with NO_x-sensitive and VOC-sensitive chemistry and with previous measurements. Indicator measurements provide valid information about O_3-NO_x-VOC sensitivity only if they show a correlation pattern that is consistent with results from either NO_x-sensitive or VOC-sensitive models. If measurements fail to show this agreement, than the ratios are not valid as NO_x-VOC indictors. This is described below.

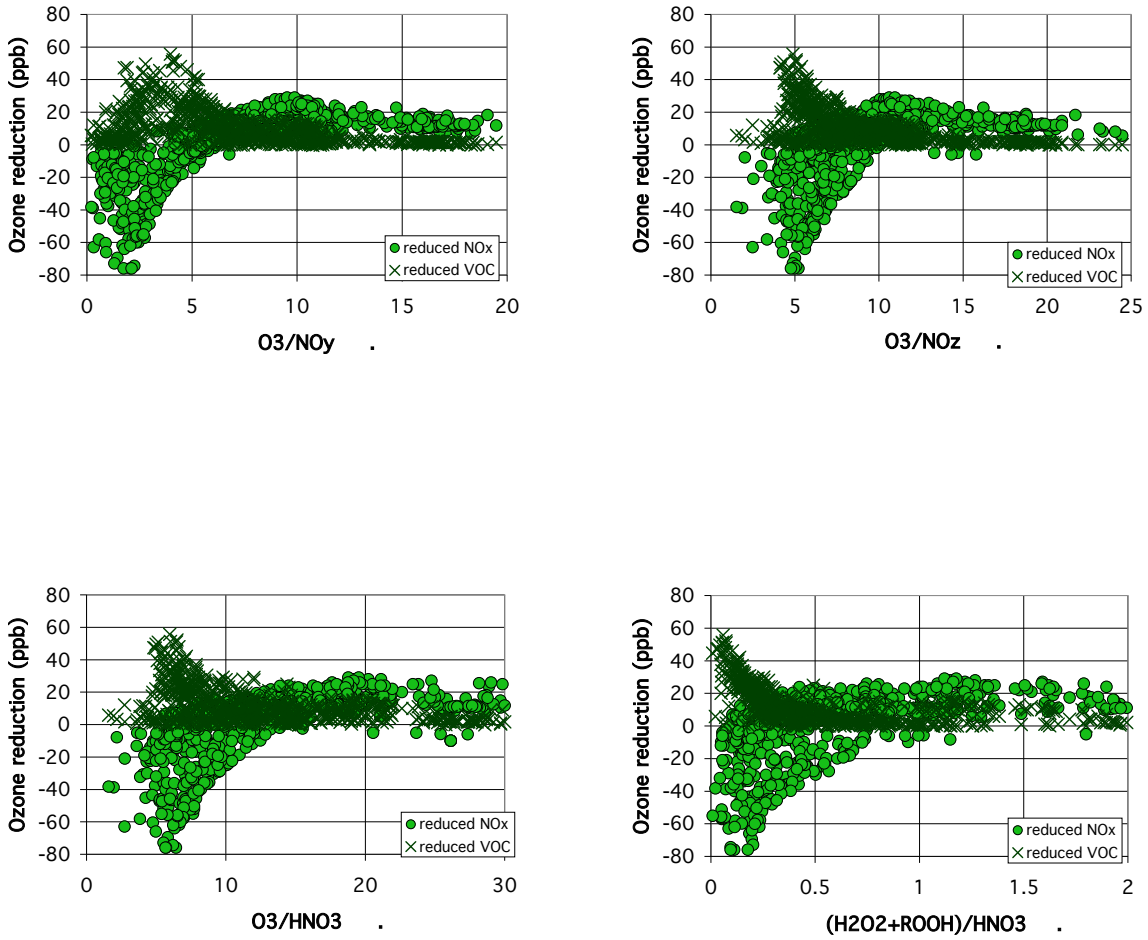

Figure 2.1. Predicted reductions in ozone in response to a percent reduction in emissions of anthropogenic VOC (crosses), and predicted reductions in response to the same percent reduction in emissions of anthropogenic NO_x (green circles), plotted versus model values for proposed indicator ratios: O_3/NO_y, O_3/NO_z, O_3/HNO_3, and $(H_2O_2+ROOH)/HNO_3$. Results are shown for four separate model scenarios (Lake Michigan, northeast, Nashville, and Los Angeles, from Table 2.1). Percent reductions are either 25% or 35% in individual scenarios.

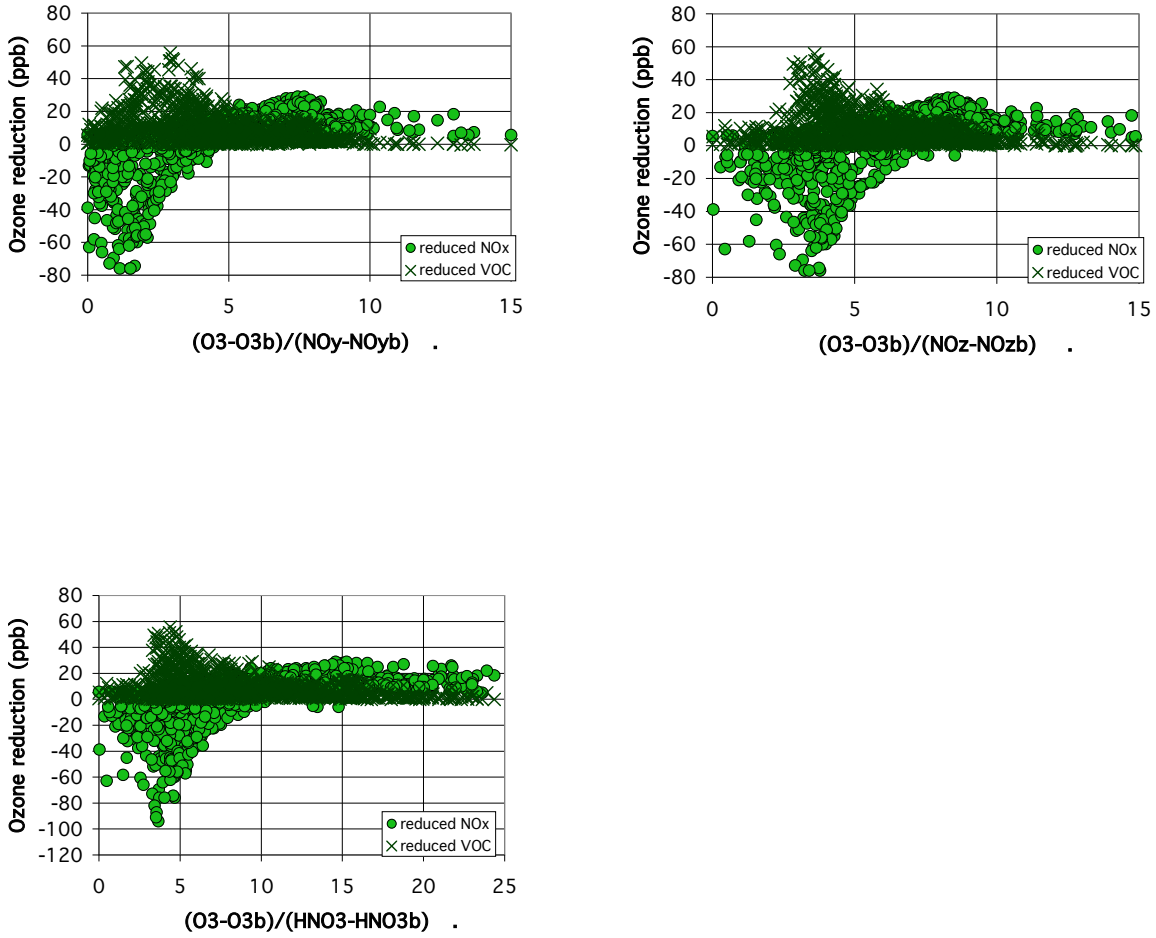

Figure 2.1 (continued). Predicted reductions in ozone in response to a percent reduction in emissions of anthropogenic VOC (crosses), and predicted reductions in response to the same percent reduction in emissions of anthropogenic NO_x (green circles), plotted versus model values for proposed indicator ratios: $(O_3\text{-}O_{3b})/(NO_y\text{-}NO_{yb})$, $(O_3\text{-}O_{3b})/(NO_z\text{-}NO_{zb})$, and $(O_3\text{-}O_{3b})/(HNO_3\text{-}HNO_{3b})$. Results are shown for five separate model scenarios (see Table 2.1). Percent reductions are either 25% or 35% in individual scenarios.

Table 2.1

3-d simulations used in Figure 2.1

Location	Model	Photochemistry	Model Domain	Comparison w/ measurements	Reference
Nashville	Sillman et al., 1998	modified Lurmann et al., 1986	5x5 km urban; upwind domains incl eastern U.S	O_3, NO_y, peroxides	Sillman et al., 1998
Lake Michigan	Sillman et al., 1993	modified Lurmann et al., 1986	20x20 km in region; upwind domains includes eastern U.S	O_3	Sillman, 1995
Northeast corridor	Sillman et al., 1993	modified Lurmann et al.,	20x20 km in region; upwind domains includes eastern U.S	O_3	Sillman, 1995
Atlanta	UAM-IV, Morris and Myers, 1990	CB4 (Gery et al., 1989)	5x5 km urban	O_3, NO_y, isoprene, HCHO, other VOC	Sillman et al., 1997
San Joaquin (Sillman)	MAQSIP (Odman and Ingram, 1996)	CB4 (Gery et al., 1989)	12x12 km; domain includes all central California	O_3	Sillman et al., 2001
Los Angeles (Godowitch)	UAM-IV, Morris and Myers, 1990	CB4 (Gery et al., 1989)	5x5 km urban	O_3, NO_y, NO_z	Godowitch et al. 1994; Sillman et al., 1997

Table 2.2

Values of indicator ratios for NOx-sensitive, transitional, and VOC-sensitive conditions

The VOC-sensitive and NO_x-sensitive values represent typical values for strongly VOC-sensitive and strongly NO_x--sensitive locations, derived from chemistry/transport models. Ratios lower than the transition values generally correspond to VOC-sensitive conditions. Ratios higher than the transition values generally correspond to NO_x-sensitive conditions.

indicator	median VOC-sensitive	transition	median NO_x-sensitive
O_3/NO_y	5	6-8	11
O_3/NO_z	6	8-10	14
O_3/HNO_3	9	12-15	20
$(O_3-O_3b)/(NO_y-NO_yb)$	3	3.5-5	6
$(O_3-O_3b)/(NO_z-NO_zb)$	4	5-6	7
$(O_3-O_3b)/(HNO_3-HNO_3b)$	5	7-10	12
H_2O_2/HNO_2	.15	.25-.35	.6
total peroxides/HNO_3	.2	.2-.5	.9
H_2O_2/NO_z	.12	.2-.25	.4
total peroxides/NO_z	.15	.25-.35	.7
H_2O_2/NO_y	.08	.12-.17	.35
total peroxides/NO_y	.12	.20-,25	.6

==========

2.3. Correlations among indicator species: Ozone and reactive nitrogen.

Models: Chemistry-transport models predict distinct patterns of correlation between O_3 and NO_y, between O_3 and NO_z, and between O_3 and HNO_3. These patterns are different for NO_3-sensitive and VOC-sensitive conditions.

Figure 2.2 shows O_3 vs. NO_y, O_3 vs. NO_z, and O_3 vs. HNO_3 from simulations for several cities in the U.S. (listed in **Table 2.1**), afternoon hours only. The results are sorted based on predicted O_3-NO_x-VOC sensitivity at the time and location corresponding to the ambient value. They are sorted as NO_x-sensitive, VOC-sensitive, mixed, or dominated by NO_x titration (see **Definition** below).

NO_x-sensitive locations all show a strong correlation between O_3 and NO_y, between O_3 and NO_z, and between O_3 and HNO_3, with a steep slope.

VOC-sensitive locations also show a correlation between O_3 and NO_z, and between O_3 and HNO_3, but the range of values is different and the slope is lower. VOC-sensitive locations may also have a positive correlation between O_3 and NO_y or they may have little or no correlation between O_3 and NO_y.

This figure is also available as a **data file** [http://www-personal.engin.umich.edu/~sillman].

Figure 2.3 shows correlation patterns for O_3 vs. NO_y in individual simulations. These may look different from the composite correlation pattern. It is important to recognize that even a VOC-sensitive simulation may have a strong correlation between O_3 and NO_y (e.g. Lake Michigan).

2.3a. Definition: NO_x-VOC sensitivity: Locations are defined as ***NO_x-sensitive*** if a percent (25%-50%) reduction in NO_x emissions would cause a significant (>5 ppb) reduction in O_3, and if the resulting O_3 is significantly lower than would result from the same percent reduction in anthropogenic VOC. Locations are defined as ***VOC-sensitive*** if a percent reduction in VOC would cause a significant reduction in O_3, and if the resulting O_x is significantly lower than would result from the same percent reduction in NO_x. Locations are defined as **mixed** if a percent reduction in NO_y would not result in O_3 that is significantly higher or significantly lower than the same percent reduction in VOC. Locations are defined as **dominated by NO_y titration** if a percent reduction in NO_y would cause a significant increase in O_3, while a percent reduction in VOC would not cause a significant reduction in O_3.

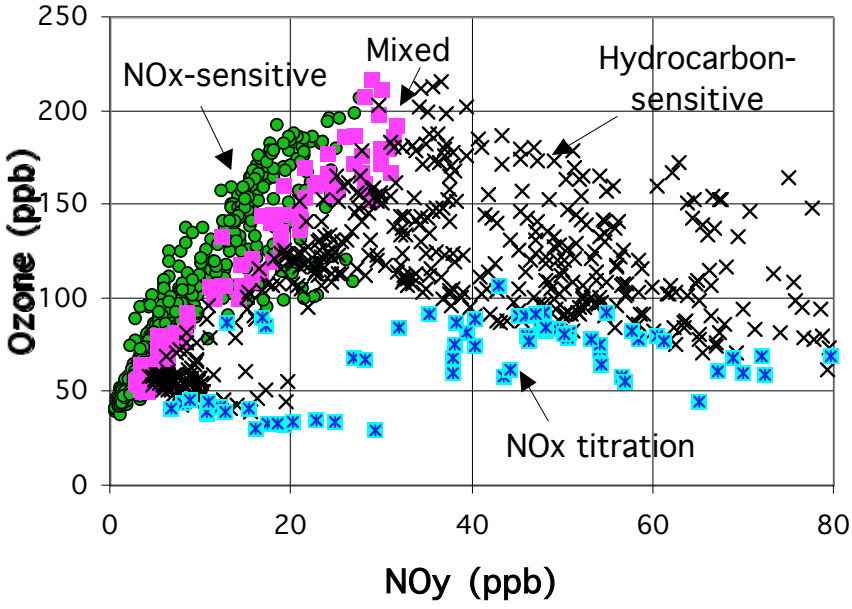

(a)

Figure 2.2 . Correlations for (a) O_3 vs. NO_y, (b) O_3 vs. NO_z, and (c) O_3 vs. HNO_3 vs. HNO_3 (all in ppb) from the 3-d simulations listed in **Table 2.1**. Each location is classified as NO_x-sensitive (green circles), VOC-sensitive (crosses), mixed or with near-zero sensitivity (lavender squares), and dominated by NOx titration (blue asterisks) based on definitions in the text. From Sillman and He (2002). This figure is also available as a **data file** [http://www-personal.engin.umich.edu/~sillman].

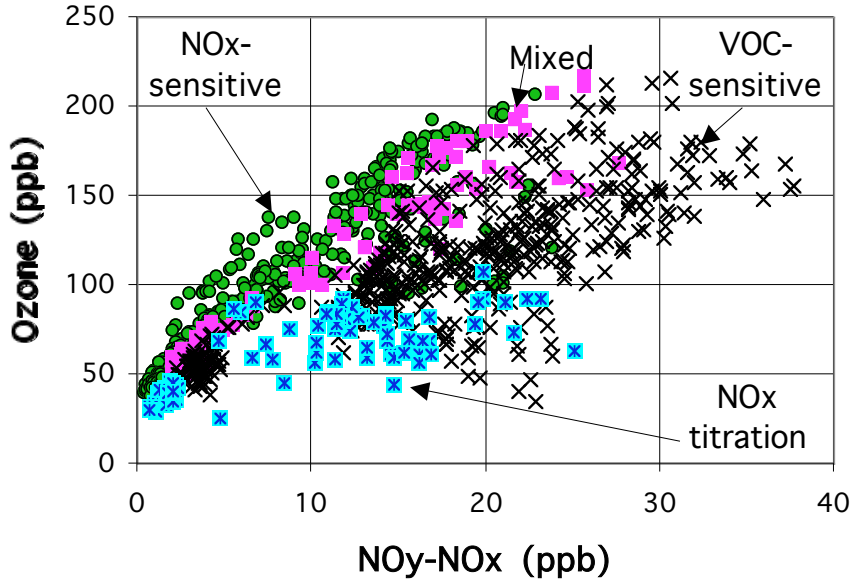

(b)

Figure 2.2. Correlations for (a) O_3 vs. NO_y, (b) O_3 vs. NO_z, and (c) O_3 vs. HNO_3 (all in ppb) from the 3-d simulations listed in Table 3.1.1. Each location is classified as NO_x-sensitive (green circles), VOC-sensitive (crosses), mixed or with near-zero sensitivity (lavender squares), and dominated by NOx titration (blue asterisks) based on definitions in the text. From Sillman and He (2002). This figure is also available as a **data file** [http://www-personal.engin.umich.edu/~sillman].

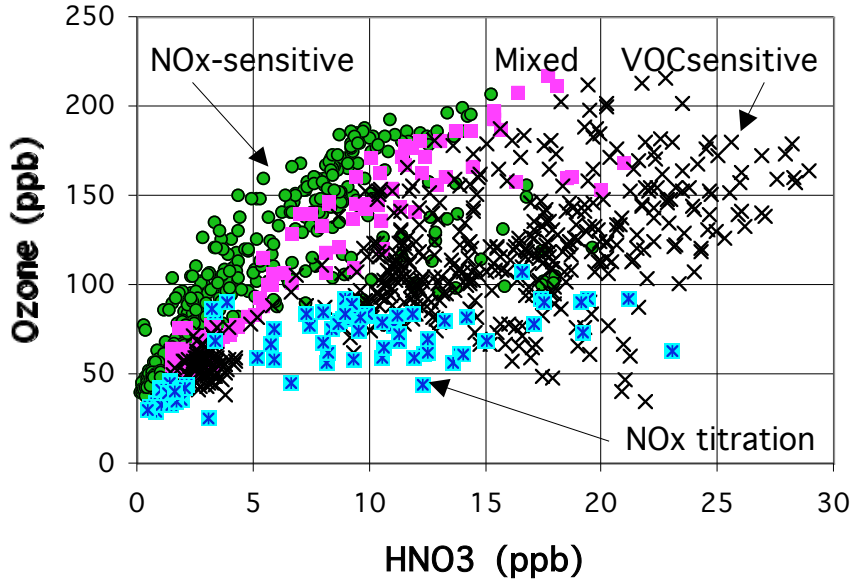

(c)

Figure 2.2. Correlations for (a) O_3 vs. NO_y, (b) O_3 vs. NO_z, and (c) O_3 vs. HNO_3 (all in ppb) from the 3-d simulations listed in Table 3.1.1. Each location is classified as NO_x-sensitive (green circles), VOC-sensitive (crosses), mixed or with near-zero sensitivity (lavender squares), and dominated by NOx titration (blue asterisks) based on definitions in the text. From Sillman and He (2002). This figure is also available as a **data file** [http://www-personal.engin.umich.edu/~sillman].

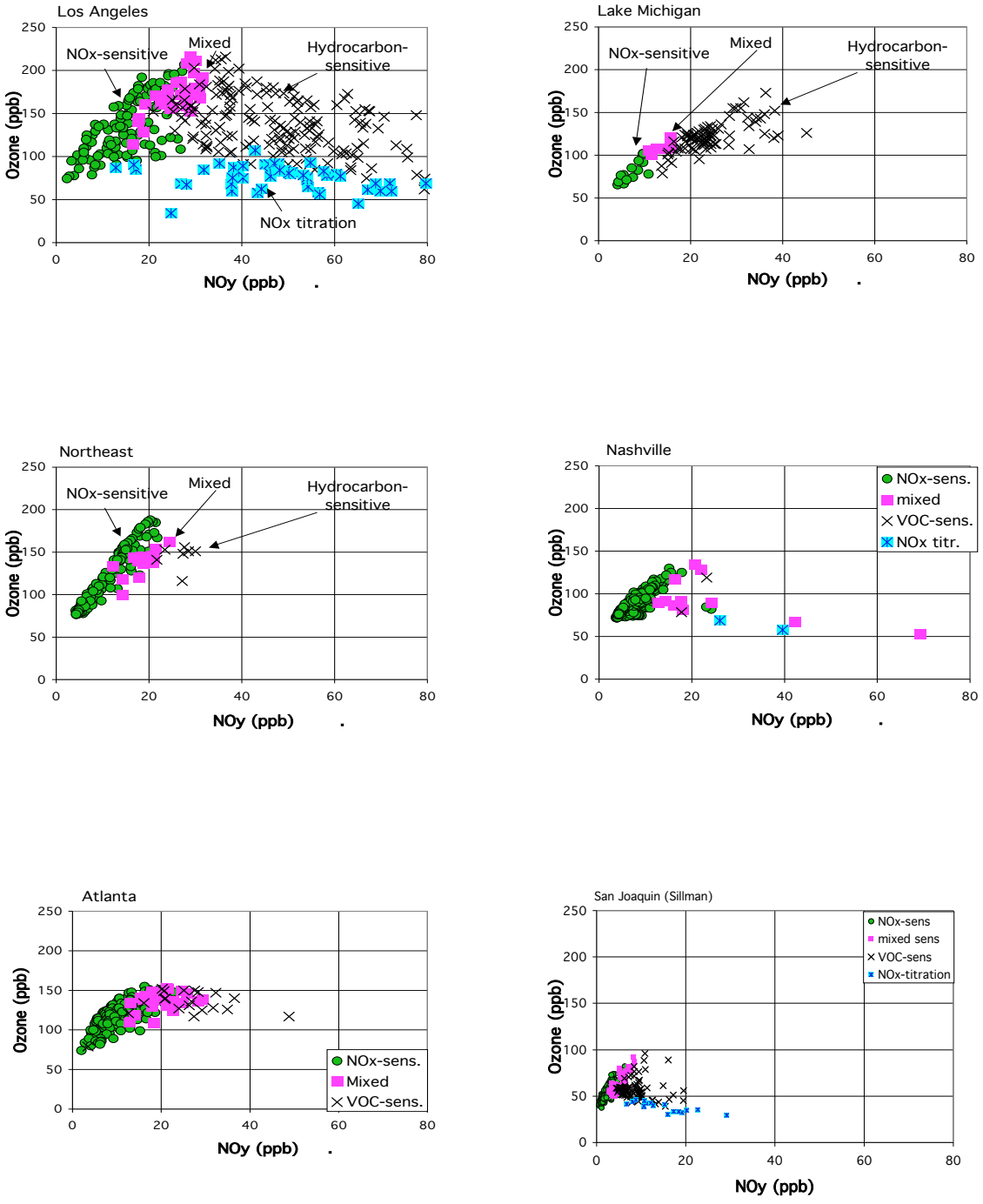

Figure 2.3. Correlations for O_3 vs. NO_y in ppb from individual 3-d simulations listed in Table 3.1.1. Each location is classified as NO_x-sensitive (green circles), VOC-sensitive (crosses), mixed or with near-zero sensitivity (lavender squares), and dominated by NOx titration (blue asterisks) based on definitions in the text. Models are (a) Los Angeles (Godowitch), (b) Lake Michigan, (c) northeast corridor, (d) Nashville, (e) Atlanta, and (f) San Joaquin (Lu and Chang).

Measurements for O_3 vs. NO_z show a range of correlation patterns that is similar to model values. These are shown in **Figure 2.4**.

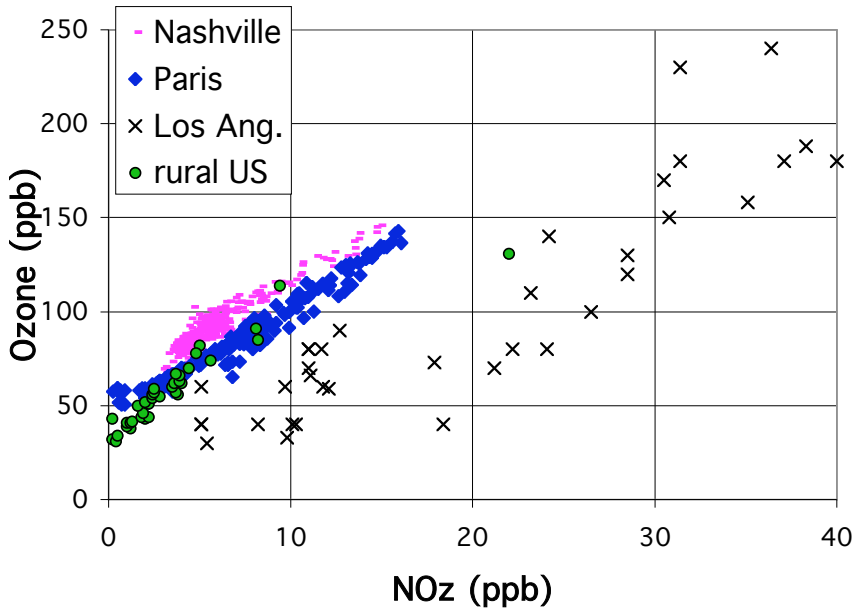

(b)

Figure 2.4. Measured correlations between O_3 and NO_Z, both in ppb. Measurements are shown from field campaigns in Nashville (pink dashes), Paris (blue diamonds), Los Angeles (X's) and from four rural sites in the eastern U.S. (green circles). From measurements reported by Sillman et al., 1997, 1998, 2002 and Trainer et al., 1993.

==========

2.4. Model-measurement comparisons: Ozone and reactive nitrogen

Model-measurement comparisons for ozone and reactive nitrogen provide a way to evaluate the accuracy of models and also to evaluate whether measurements can properly be interpreted as evidence for NO_x-VOC sensitivity.

The two critical evaluations are: (i) full-domain correlations between O_3 and NO_z, etc. (afternoon values only); and (ii) indicator species values associated with peak and near-peak O_3.

Here are examples.

A primarily NO_x-sensitive model: Nashville (Figure 2.5). Model and measured O_3 vs. NO_z both show a strong positive correlation. The range of values of O_3 and NO_z are similar in the model and in measurements. Peak O_3 and NO_z associated with peak O_3 in the model differ from the measured peak O_3 and associated NO_z by 10% or less, suggesting good model-measurement agreement. The ratio O_3/NO_z associated with peak O_3 is lower in the model than in measurements by 15% (8.4 model, 9.7 measurements). This difference is too small to suggest bias in model NO_x-VOC sensitivity predictions.

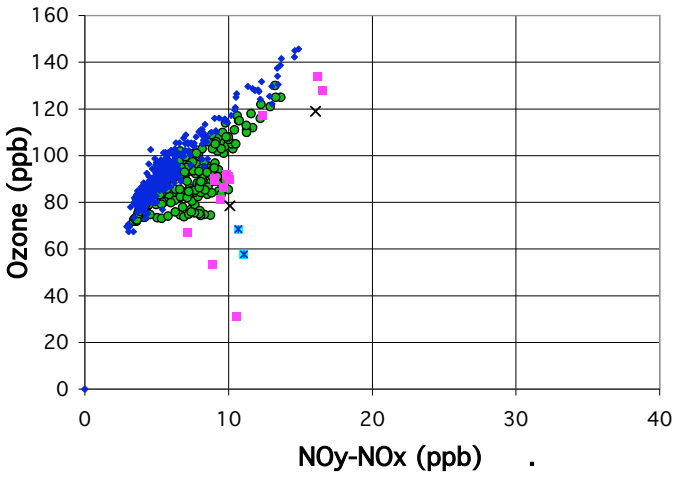

Figure 2.5. Measured correlation between O_3 and NO_Z (ppb) (blue diamonds), compared with model results for Nashville (Sillman et al., 1998). Each model location is classified as NO_X-sensitive (green circles), VOC-sensitive (crosses), mixed or with near-zero sensitivity (lavender squares), and dominated by NOx titration (blue asterisks) based on definitions in the text.

A VOC-sensitive model: Los Angeles (Figure 6). The model scenario shows a positive correlation between O_3 and NO_z, but with scatter, and with mostly VOC-sensitive chemistry. Measurements also show a positive correlation with scatter, and with a similar range of O_3 vs. NO_z, The measurements correspond closely to model values that are associated with VOC-sensitive conditions. The model also shows some NO_x-sensitive locations, but very few measurements correspond to the NO_x-sensitive O_3 vs. NO_z in the model. The model predicts peak O_3 with both mixed and VOC-sensitive conditions. Peak O_3 is underestimated by 10% vs. measurements, but NO_z and O_3/NO_z are both underestimated by approximately 30%. The difference between model and measured O_3/NO_z at peak O_3 (7.9 model, 6.0 measured) corresponds to the difference between somewhat VOC-sensitive conditions and strongly VOC-sensitive conditions in **Figure 2.1**. This suggests that the model scenario, though primarily VOC-sensitive, may still be somewhat biased towards NO_x-sensitive chemistry.

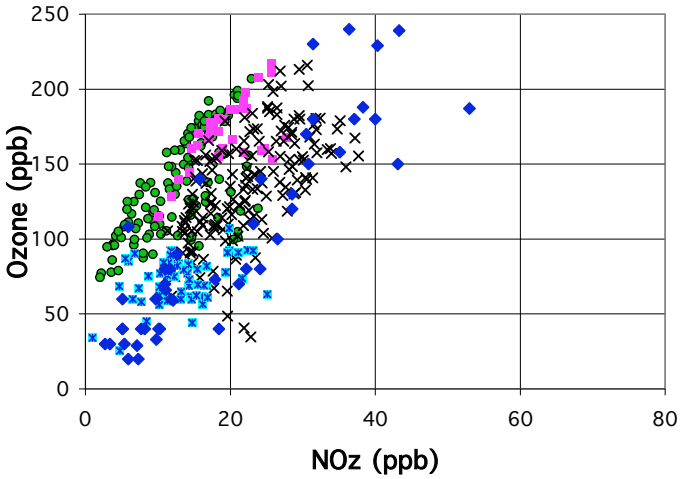

Figure 2.6. Measured correlation between O_3 and NO_Z (ppb) (blue diamonds), compared with model results for Los Angeles (Sillman et al., 1997). Each model location is classified as NO_X-sensitive (green circles), VOC-sensitive (crosses), mixed or with near-zero sensitivity (lavender squares), and dominated by NOx titration (blue asterisks) based on definitions in the text.

A biased model: Atlanta (Figure 7): The first model scenario (Figure 7a) predicts VOC-sensitive conditions associated with peak O_3 in the Atlanta urban plume and NO_x-sensitive conditions elsewhere. Measured O_3 vs. NO_3 agrees with the model values for NO_x-sensitive regions of the model, but disagree with model values for VOC-sensitive regions only. Model peak O_3 is in good agreement with measured peak O_3, but NO_y and O_3/NO_y in the vicinity of peak O_3 are both higher in the model than in measurements by nearly a factor of two.

A modified model scenario with strongly NO_x-sensitive conditions (Figure 5b) shows better agreement with measurements. Model peak O_3, NO_y and O_3/NO_y in the vicinity of peak O_3, all are within 15% of measured values.

In this evaluation, the VOC-sensitive and NO_x-sensitive model scenarios both show good agreement with measured O_3. An evaluation using O_3 vs. NO_y is necessary to identify model errors.

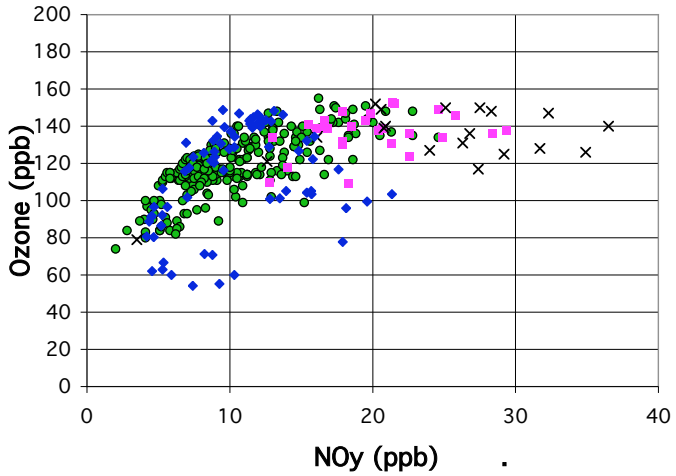

(a)

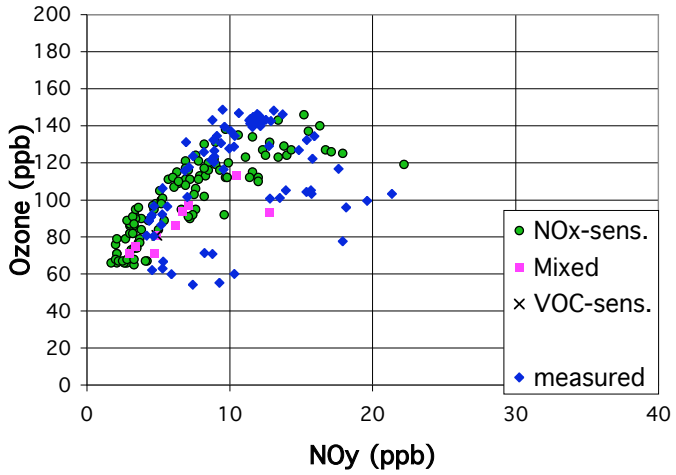

(b)

Figure 2.7. Measured correlation between O_3 and NO_Z (ppb) (blue diamonds), compared with model results for Atlanta (Sillman et al., 1997). Each model location is classified as NO_X-sensitive (green circles), VOC-sensitive (crosses), mixed or with near-zero sensitivity (lavender squares), and dominated by NOx titration (blue asterisks) based on definitions in the text.

An event where indicators are invalid: (unpublished data, Figure 2.8): Here, measured O_3 vs. NO_z differs from model values for the whole model domain. The measured O_3 vs. NO_z does not correspond to model results for either NO_x-sensitive or VOC-sensitive cases. This type of model-measurement discrepancy might be caused by one of several factors: loss of reactive nitrogen through wet deposition or through aerosol interactions, unknown photochemical processes, or erroneous measurements. Based on this model-measurement discrepancy, it is not valid to draw inferences about O_x-NO_x-VOC sensitivity from the measurements.

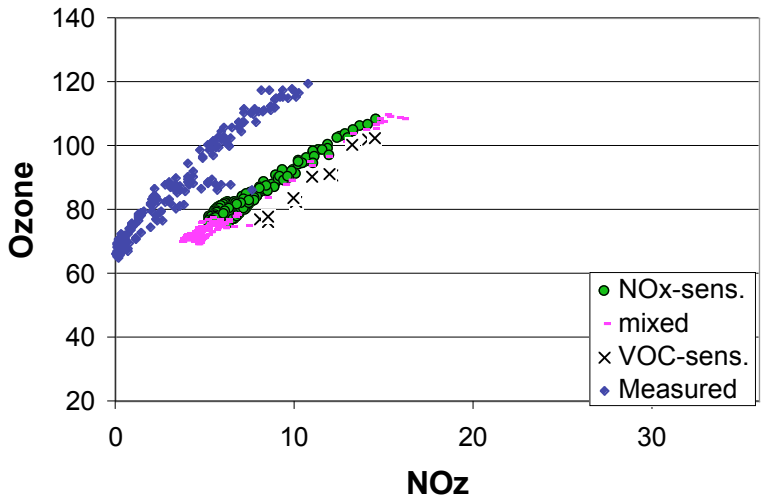

Figure 2.8. Measured correlation between O_3 and NO_Z (ppb) (blue diamonds), compared with model results for Paris (unpublished). Each model location is classified as NO_X-sensitive (green circles), VOC-sensitive (crosses), mixed or with near-zero sensitivity (lavender squares), and dominated by NOx titration (blue asterisks) based on definitions in the text.

==========

2.5. Other species: Organic nitrates and peroxides.

2.5.1. Ozone vs organic nitrates:

The correlation between O_3 and organic nitrates (**Figure 2.9**) is completely unrelated to O_3-NO_x-VOC sensitivity. As shown in the Figure 9, the correlation between O_3 and organic nitrates is the same for both NO_x-sensitive and VOC-sensitive conditions.

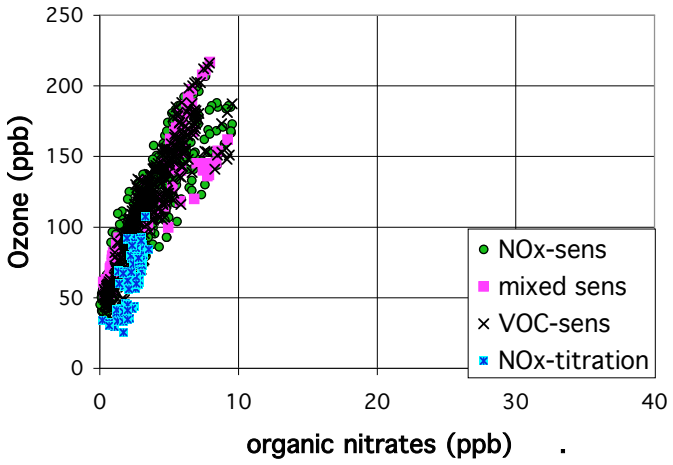

Figure 2.9. Correlations for organic nitrates (defined as NO_y-NO_X-HNO_3, in ppb) from the 3-d simulations listed in **Table 2.1**. Each location is classified as NO_X-sensitive (green circles), VOC-sensitive (crosses), mixed or with near-zero sensitivity (lavender squares), and dominated by NOx titration (blue asterisks) based on definitions in the text.

2.5.2. Peroxides: If measured H_2O_2 and/or organic peroxides are available, a much stronger evaluation of model accuracy can be provided.

Models predict that peroxides vs. HNO_3 show a very different range of values for NO_x-sensitive and VOC-sensitive conditions. (**Figure 2.10**).

There is no predicted correlation between peroxides and HNO_3 or between peroxides and NO_z. However, models predict a strong, consistent correlation between O_3 and the sum $2H_2O_2$+NO_z **(Figure 2.11)**. This correlation is similar for both NO_x-sensitive and VOC-sensitive conditions and provides a test for general validity of indicator ratios.

When measurements agree with model values for this correlation, it guarantees that the indicator ratios O_3/NO_z and $2H_2O_2/NO_z$ are consistent with each other – both ratios will suggest the same O_3-NO_x-VOC sensitivity. Errors that would invalidate indicator ratios (e.g. removal of HNO_3 through wet deposition or aerosol interactions) would also cause a model-measurement discrepancy for O_3 vs. $2H_2O_2$+NO_z.

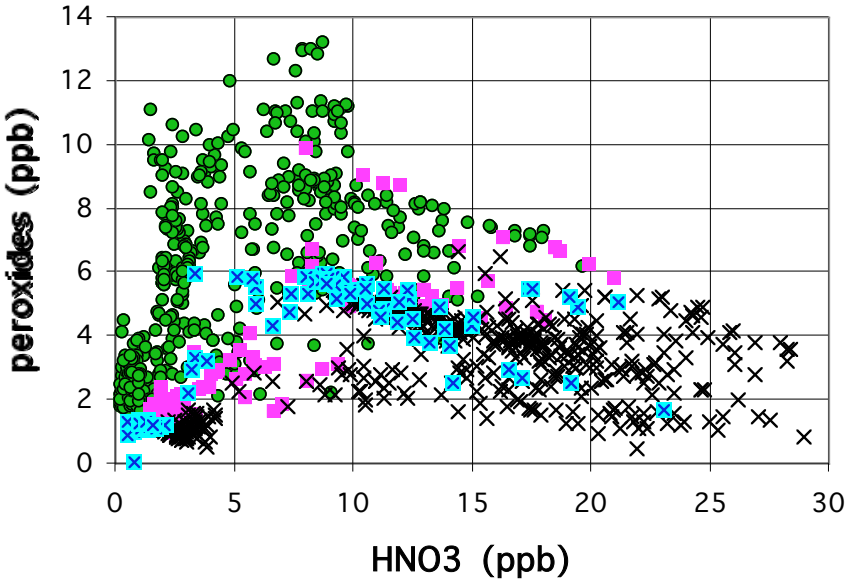

Figure 2.10 . Correlations for total peroxides vs. HNO_3 (in ppb) from the 3-d simulations listed in **Table 2.1**. Each location is classified as NO_X-sensitive (green circles), VOC-sensitive (crosses), mixed or with near-zero sensitivity (lavender squares), and dominated by NOx titration (blue asterisks) based on definitions in the text. From Sillman and He (2002).

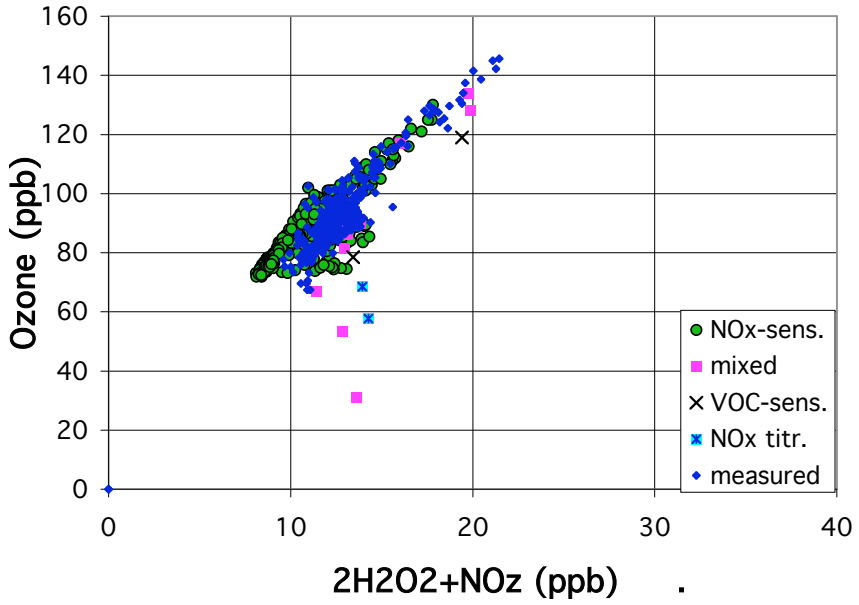

Figure 2.11. Measured correlation between O_3 and the sum $2H_2O_2+NO_Z$ (ppb) in Nashville (blue diamonds), compared with model results. Each model location is classified as NO_X-sensitive (green circles), VOC-sensitive (crosses), mixed or with near-zero sensitivity (lavender squares), and dominated by NOx titration (blue asterisks) based on definitions in the text. The model and measurements are from Sillman et al. (1998).

==========

2.6. Practical implementation.

Use of indicator ratios to evaluate O_3-NO_x-VOC sensitivity requires a network of measured O_3 and either NO_y or HNO_3. The value NO_z is derived from measured NO_y and NO_x.

The network must be extensive enough to include the region with the likely peak O_3. Measured secondary species only would provide information about conditions at the measurement site.

The measured total reactive nitrogen (NO_y) must include gas-phase HNO_3. It is not possible to substitute NO_x or the sum of NO_x and organic nitrates (supplied by some types of instruments associated with the PAMS network) for NO_y. As described elsewhere, the connection between NO_y and O_3-NO_3-VOC sensitivity is primarily due to HNO_3 rather than to other components of NO_y. It is also important to insure that HNO_3 is not lost in the inlet tubes of the NO_y instrument. ((Luke et al., 1998, Parrish et al., 2000 and McClenny et al., 2000 provide information about this.)

Results should be evaluated separately on a day-to-day basis. Measurements affected by rainfall events (at the site or upwind) cannot be used as NO_y-VOC indicators because HNO_3 has been removed. This situations can sometimes be identified by analyzing measurements on a day-by-day basis.

Measured O_3 versus NO_y (or NO_z or HNO_3) should be plotted and tabulated for the afternoon hours only (12 noon to 2 hours before sunset). Values during the evening are likely to be affected by surface deposition, and different correlation patterns are expected during the morning.

The correlation between O_3 and NO_y, etc. should be superimposed on the pattern of model correlations for NO_y-sensitive and VOC-sensitive conditions (**Figure 2.2**, also available as a **data file** [Link: **O3NOy-model-results**].) and/or measurements. To be valid, measured values should fall within the broad range of model values. If a significant portion of measurements fall outside the range of model values, then the measurements for the day in question should not be interpreted as NO_y-VOC indicators.

Model-measurement comparisons for O_3 and NO_y, etc. should include both a general evaluation and an evaluation for peak and near-peak O_3. This should be based on afternoon values only. They should include the complete ensemble of measurement sites within a metropolitan area, and use model ambient concentrations for the same times and locations of the measurements.

Model and measured ensemble correlations should be plotted for each day, as in **Figures 2.5-2.8**. It is useful to plot model correlations for both the entire model domain and for the measurement sites only, in order to identify whether the measurement sites are representative of conditions throughout the area of interest.

The following procedure is suggested:

- **Peak O_3**: Identify model NO_y (or NO_z or HNO_3) and the ratio O_3/NO_y at the time and place of model peak O_3, and measured NO_y and O_3/NO_y, etc. at the time and place of measured peak O_3.

- **Near-peak O_3**: Identify the model mean NO_y (or NO_z or HNO_3) and range of NO_y values for times and locations with model O_3 within 10% of the model peak value, and identify the measured mean NO_y (or NO_z or HNO_3) and range of values for times and locations with measured O_3 within 10% of the measured peak value,

- **General correlation**: Establish a series of intervals for the afternoon values of NO_y, NO_z or HNO_3, based on the range of afternoon values in the model and in measurements: 0-2 ppb, 2-4, 4-6, 6-8, etc. Identify mean O_3 for all model locations with NO_y (or NO_z or HNO_3) in the specified interval and for all measurements with NO_y in the specified interval. These values will be used for a model-measurement comparison.

Interpretation:

- Assuming reasonable overall agreement, the model NO_y (or NO_z or HNO_3) and indicator ratio values associated with peak O_3, and the range of model NO_y, etc. for near-peak O_3, should all agree with measured values to within 25%. (The 25% represents the uncertainty in photochemical calculations, from Gao et al., 1996.)

  This is a critical test, which can identify bias in what otherwise seems like a good model-measurement agreement. (For examples, see the discussion associated with **Figures 2.6** and **2.7**.)

- Model-measurement comparisons associated with peak O_3 are meaningful only if the model shows reasonable agreement with measurements over the full range of NO_y (or NO_z or HNO_3). If the model consistently underpredicts or overpredicts O_3 relative to NO_y (or NO_z or HNO_3) relative to measurements over the full range of values (as in **Figure 2.8**), then the measurements should be rejected as having meaning for evaluating NO_x-VOC sensitivity.

- Model and measurements should show reasonable agreement for low values of NO_y (or NO_z or HNO_3), representing relatively clean conditions. If models and measurements disagree for clean conditions, it suggests errors in the model boundary condition.

- Mean measured O_3 should be within 25% of model O_3 for each interval of NO_y (or NO_z or HNO_3).

- Some leeway can be allowed in model vs. measured indicator ratios associated with peak O_3 if the model and measured values both suggest the same O_3-NO_x-VOC sensitivity. If model and measured indicator ratios are both clearly in the NO_x-sensitive range or clearly in the VOC-sensitive range as identified in **Figure 2.1** and **Table 2.2**, then discrepancies larger than 25% at peak O_3 may be tolerated.

==========

3. SMOG PRODUCTION ALGORITHMS (EXTENT OF REACTION PARAMETERS).

Smog production algorithms are **not** recommended for use here. Results shown here identify weaknesses in the method. For a more positive view, refer to Blanchard et al. (1999), Blanchard (2000) and Blanchard and Stockenius (2001).

The smog production algorithms consist of "extent of reaction parameters", which are calculated as function of either (i) ambient O_3 and NO_y, (ii) NO_x and NO_y, or (iii) O_x and NO_x. A low extent of reaction (<0.6) suggests the presence of largely unprocessed direct emissions, and is interpreted as VOC-sensitive. A high extent of reaction (>0.9) suggests that photochemistry has been run to completion, and is interpreted as NO_x-sensitive.

The following are weaknesses in the smog production algorithms.

Rule of thumb: The smog production algorithms consist only of rules of thumb, intended to tell whether ambient O_3 is primarily sensitive to NO_x or to VOC based on field measurements. They have never been linked to a broader analysis of ambient measurements that might evaluate the appropriateness of the method.

Reliance on smog chamber results: The smog production algorithms were derived empirically from results of smog chamber experiments. This is an advantage in one sense: the algorithms are not dependent on model calculations. However, they differ from ambient conditions in many ways.

- Smog chambers typically include a single rapid introduction of precursors, rather than continuous and varying precursor emissions as occur in nature.

- Smog chambers typically have VOC and NOx concentrations that are much higher than ambient concentrations at times of high ozone production.

- Smog chambers do not include multi-day processes.

- Dry deposition in smog chambers is very different from dry deposition outdoors.

Conceptual flaws: The central concept is that NO_x-sensitive conditions are associated with a high "extent of reaction" - photochemically aged air that has had most of its NOx reacted away. VOC-sensitive conditions are associated with a low "extent of reaction", including relatively fresh emissions.

Relatively fresh emissions are in fact more likely to have VOC-sensitive photochemistry, and aged downwind emissions are more likely to be NO_x-sensitive (Milford et al., 1989, 1994). But this is not universally true, and there is no causal link.

Photochemically aged air can still be primarily VOC-sensitive if emission sources have low VOC/NOx ratios, low VOC reactivity, and little or no biogenic VOC. Ambient measurements have identified instances of photochemically aged air with apparently VOC-sensitive chemistry (Jacob et al., 1995, Hirsch et al., 1996, Kleinman et al., 2002). Such cases have also been found in chemistry-transport models. See, for example, the Lake Michigan case in **Figure 2.3**.

Relatively fresh emissions can be primarily NOx-sensitive if they have high VOC/NOx ratios and high VOC reactivity.

Results from chemistry/transport models: **Figure 3.1** shows how predicted O_3-NO_x-VOC sensitivity compares with extent of reaction derived from predicted ambient conditions in chemistry/transport models. This is equivalent to **Figure 2.1** for NO_x-VOC indicators, with models listed in **Table 2.1**.

Three different extent-of-reaction parameters are used, as defined by Blanchard et al. (1999). They may be represented approximately as: (i) $(O_3\text{-}O_3b)/19NO_y^{0.67}$, (ii) $(1\text{-}NO_x/NO_y)^{0.67}$, and (iii) $(O_3\text{-}O_3b)/19NO_x^{0.67}$. The complete formulas are given in the **Draft report to EPA** [available from http://www-personal.engin.umich.edu/~sillman] and in Blanchard et al., 1999.

The first extent parameter shows reasonably good agreement with O_3-NO_x-VOC sensitivity. The other parameters show worse agreement. VOC-sensitive conditions are found for almost the entire range of values of the second and third extent parameter.

The poor results are largely due to the simulation for Lake Michigan, because this simulation includes an aged urban plume from Chicago that remains VOC-sensitive as it travels downwind.

Figure 3.2 shows the same results in different format. Figure 3.2 also compares the extent parameter $(O_3\text{-}O_3b)/19NO_y^{0.67}$ with a simpler alternative, $(O_3\text{-}O_3b)/(NO_y\text{-}NO_yb)$. The simpler alternative (included above as a NO_x-VOC indicator) gives better results.

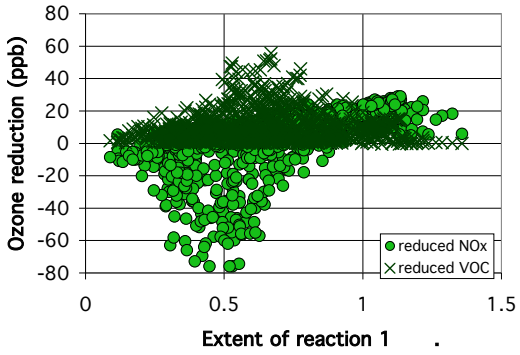
Ozone reduction (ppb)
80
60
40
20
0
-20
-40
-60
-80
0
0.5
1
1.5
reduced NOx
reduced VOC
Extent of reaction 1

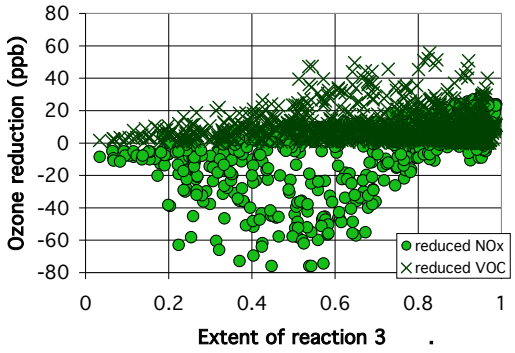
Ozone reduction (ppb)
80
60
40
20
0
-20
-40
-60
-80
0
0.2
0.4
0.6
0.8
1
reduced NOx
reduced VOC
Extent of reaction 3

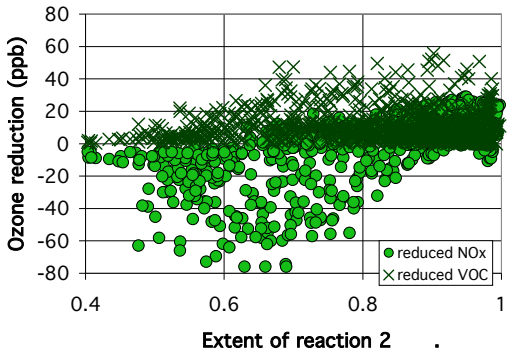
Ozone reduction (ppb)
80
60
40
20
0
-20
-40
-60
-80
0.4
0.6
0.8
1
reduced NOx
reduced VOC
Extent of reaction 2

Figure 3.1. Predicted reductions in ozone in response to a percent reduction in emissions of anthropogenic VOC (crosses), and predicted reductions in response to the same percent reduction in emissions of anthropogenic NO_X (green circles), plotted versus model values for three extent parameters (B1, B2 and B3, defined as in Blanchard et al., 1999, and given in the **Draft Report to EPA**), for the five model scenarios from **Table 2.1**. Percent reductions are either 25% or 35% in individual scenarios. Based on results shown in Sillman and He (2002).

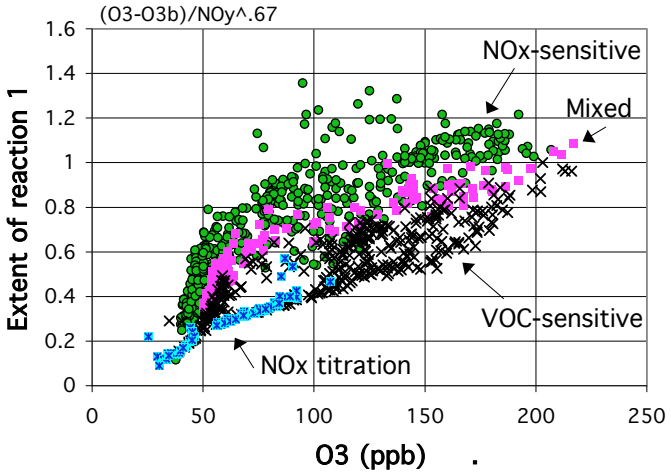

(a) ExtentB1 (Equation 3.2.3).

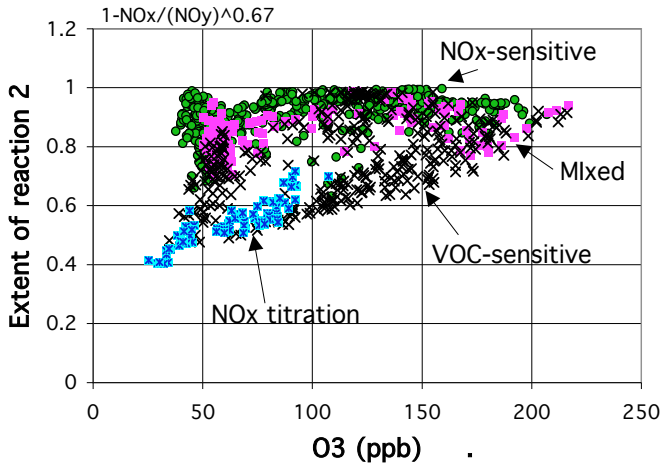

(b) ExtentB2 (Equation 3.2.5).

Figure 3.2. Extent of reaction versus O_3 for five model scenarios listed in **Table 2.1**. Each location is classified as NO_X-sensitive (green circles), VOC-sensitive (crosses), mixed or with near-zero sensitivity (lavender squares), and dominated by NOx titration (blue asterisks) based on definitions in the text. Results are shown for the three extent parameters (B1, B2 and B3, defined in Equations 3.2.3, 3.2.5 and 3.2.8 in the **Draft Report to EPA**, from Blanchard et al., 1999). Results for the ratio $(O_3\text{-}O_{3b})/(NO_y\text{-}NO_{yb})$ are shown for comparison. From Sillman and He (2002).

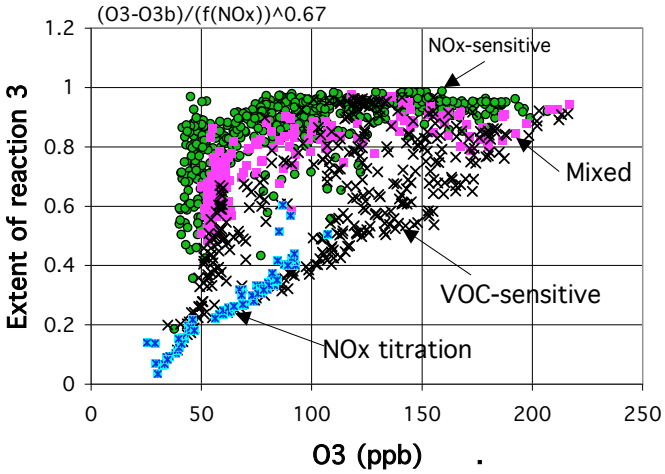

(c) ExtentB3 (Equation 3.2.8).

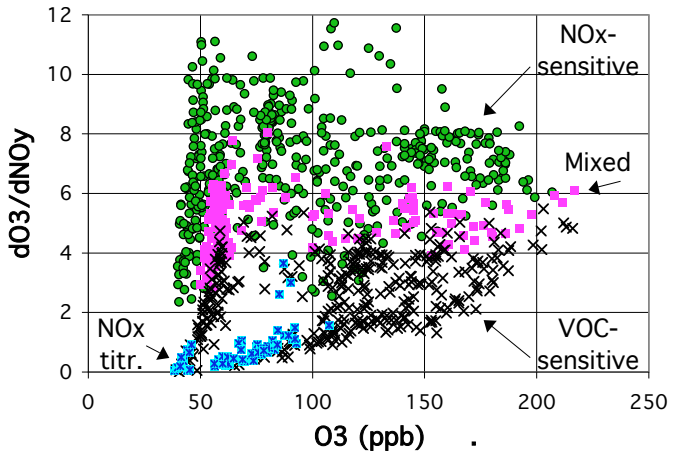

(d) $(O_3\text{-}O_{3b})/(NO_y\text{-}NO_{yb})$

Figure 3.2. Extent of reaction versus O_3 for five model scenarios listed in **Table 2.1**. Each location is classified as NO_x-sensitive (green circles), VOC-sensitive (crosses), mixed or with near-zero sensitivity (lavender squares), and dominated by NOx titration (blue asterisks) based on definitions in the text. Results are shown for the three extent parameters (B1, B2 and B3, defined in Equations 3.2.3, 3.2.5 and 3.2.8 in the **Draft Report to EPA**). Results for the ratio $(O_3\text{-}O_{3b})/(NO_y\text{-}NO_{yb})$ are shown for comparison. From Sillman and He (2002).

==========

4. METHODS BASED ON AMBIENT VOC AND NO_x.

CONTENTS.

==========

4.1. Rules of thumb: ambient NO_x, VOC and O_3-NO_x-VOC sensitivity.

Ambient NO_x and VOC are directly related to the instantaneous rate of production of O_3. Given measurements of NO_x and primary hydrocarbons (along with meteorological data), it is possible to calculate the instantaneous rate of ozone production using a 0-d photochemical calculation.

Ambient NO_x and VOC are also directly related to the NO_x-VOC sensitivity of the instantaneous rate of ozone production. In particular, instantaneous NO_x-VOC sensitivity is closely related to the ratio of reactivity-weighted VOC to NO_x.

The ratio of reactivity-weighted VOC to NO_x is also related to the ratio of production rates of ozone and HNO_3, $(p(O_3)/p(HNO_3)$, and to the **ozone production efficiency**. Because of this, the ambient slope between O_3 and NO_z or between O_3 and HNO_3 is linked to the ratio of reactivity-weighted VOC to NO_x. Analyses based on ambient VOC and NO_x and analyses based on secondary species must be consistent with each other.

There is no direct way to relate ambient NO_x and VOC to NO_x-VOC sensitivity for ambient O_3 (as opposed to the instantaneous production rate of O_3). Ambient O_3 is affected chemistry and transport over an extensive upwind region. Ambient NO_x and VOC only provide information about the instantaneous production rate at the time and place of measurements.

An old rule of thumb, relating O_3-NO_x-VOC sensitivity to the ambient VOC/NO_x ratio in urban centers during the morning hours, is not correct. The old rule was based on a specific VOC speciation, omitted biogenic VOC, omitted multi-day transport, and omitted the complex geographical variation in emissions throughout a metropolitan area.

Tonnessen and Dennis (2000), Kirchner (2001) and Kleinman et al. (1997, 2000, 2001, 2002) have developed simple rules of thumb that relate the NO_x-VOC sensitivity of instantaneous production of O_3 to ambient NO_x and VOC. The rule developed by Tonnessen and Dennis (2000) and by Kirchner et al. (2001) are both equivalent to the following:

$$\text{NO}_x\text{-sensitive:} \quad \frac{\sum k_m [HC]_m}{k_a [NO_2]} > 5.7 \tag{3.1a}$$

$$\text{VOC-sensitive:} \quad \frac{\Box \sum k_m [HC]_m}{k_a [NO_2]} > 4.0 \qquad (3.1b)$$

where k_m and k_a are reaction rates for OH with individual hydrocarbons and with NO_2, and $\Box$ is an empirical correction factor (recommended as 1.3) to account for unmeasured hydrocarbons. The summation is performed over all primary and secondary hydrocarbons, and should also include oxygenated organics and CO.

(Measured VOC typically include only primary hydrocarbons and CO, with no oxygenated species. Guidance needs to be developed for the appropriate adjustment for this situation.)

Kleinman et al. (1997, 2000, 2001, 2002) developed a more complex rule that takes into account the variation in the radical source, which depends on ambient O_3 and solar radiation. They have used their rule to analyze ozone production in New York, Philadelphia, Phoenix and Houston. [These are available for download from: http://www.ecd.bnl.gov/publications.html]

Cardelino and Chameides (1995, 2000) developed a procedure for estimating overall O_3-NO_x-VOC sensitivity in a metropolitan area based on ambient NO_x and VOC. Essentially, they calculate instantaneous production rates for O_3 at all sites with measured NO_x and VOC, and use the sum to represent ozone production within the metropolitan area. Their calculation also includes procedures for including unmeasured secondary organics.

The above methods all require measurements of a relatively complete array of primary hydrocarbons, along with accurate measurements of either NO or NO_x. These measurements are not always available from the EPA PAMS network. Cardelino and Chameides (2000) found that measured NO from the PAMS network was not precise enough to provide information about NO_x-VOC sensitivity. Kleinman et al. (2000, 2001, 2002) used research-grade measurements.

These methods might also lead to erroneous results if measurement sites are affected by emissions in the immediate vicinity of the site. In addition, mixing ratios of reactive VOC such as isoprene may vary greatly with height, even within a daytime convective mixed layer (Andronache et al., 1994, Guenther et al., 1996a and b). Surface measurements may therefore not reflect the full range photochemical conditions that produce ozone.

==========

4.2. Correlations among ambient NO_x and VOC.

Parrish et al. (1998, 2000) described an analysis of measured correlations between ambient NO_x and individual VOC species, which could be used for two purposes: (i) infer **emission rates** and ratios between emissions of individual VOC and NO_x; and (ii) provide **quality assurance tests** for the accuracy and applicability of measured NO_x and VOC. This work drew on earlier findings by Goldan et al. (1995, 1997) and Buhr et al. (1992, 1995).

Species correlations as a basis for estimating emissions have been investigated in Boulder, CO (Parrish et al., 1991, Goldan et al., 1995, 1997), Nashville, TN (Goldan et al., 2001), Los Angeles (Lurmann and Main, 1992), and at rural sites in the eastern U.S. (Buhr et al., 1992, 1995).

Parrish et al. (1998) and Goldan et al. (1995, 1997) reported that correlations between individual VOC (or among individual VOC and NO_x or NO_y) with similar atmospheric lifetimes should show a slope that is equal to the ratio of emission rates among the species (**Figure 4.1**). Correlations among individual VOC with different lifetimes were more complicated.

Parrish et al. (1998, 2000) also recommended a series of tests for internal consistency among sets of measured VOC. These were based on the expected correlation between species with common origin and similar atmospheric lifetimes. They also were based on the expectation that ratios among individual VOC changed from urban centers to downwind locations in a way that reflected the relative rates of photochemical loss.

Figure 4.2 shows ratios of individual VOC relative to a reference species from measurements at sites in the U.S., in comparison with ratios among individual VOC from emission inventories. The measured ratios are often lower than the emissions ratios because photochemical removal of species tends to lower the ratio. (The reference species is the least reactive). Measurements that match very closely to the emissions ratios, even for reactive species following photochemical aging, suggest the influence of emission sources in the immediate vicinity of the measurement site (Parrish et al., 2000).

For more information on VOC internal consistency tests: Go to Parrish et al., 1998 and Parrish et al., 2000 [both available for download at http://www-personal.engin.umich.edu/~sillman].

These methods are also related to techniques of **receptor modeling** (Henry, 1994, Kim and Henry, 2000, Watson et al. 2001).

None of these methods are applicable for isoprene, because ambient isoprene is not expected to correlate with anthropogenic species.

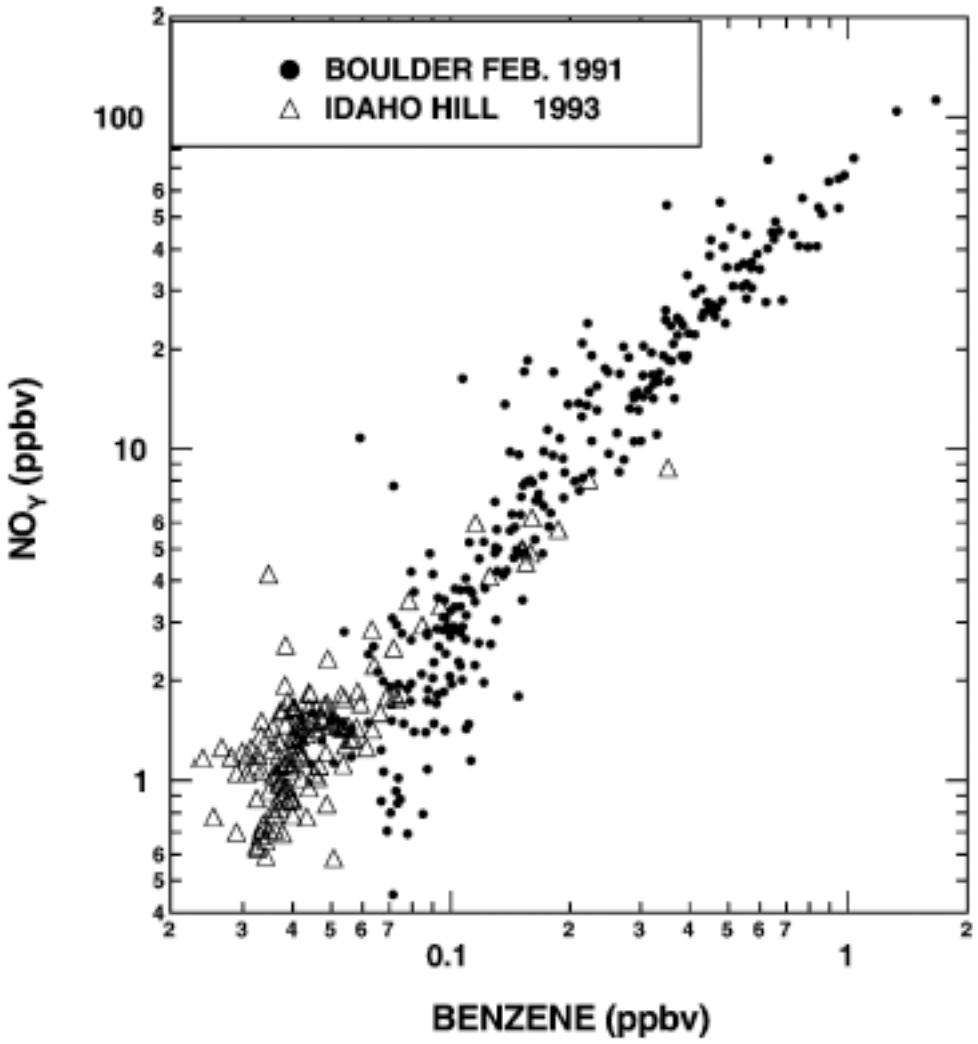

Figure 4.1. Measured correlations between Benzene and NO_y during winter at an urban site (Boulder, CO) and at a rural site (Idaho Hill, CO). From Trainer et al. (2000) based on measurements reported by Goldan et al. (1995, 1997).

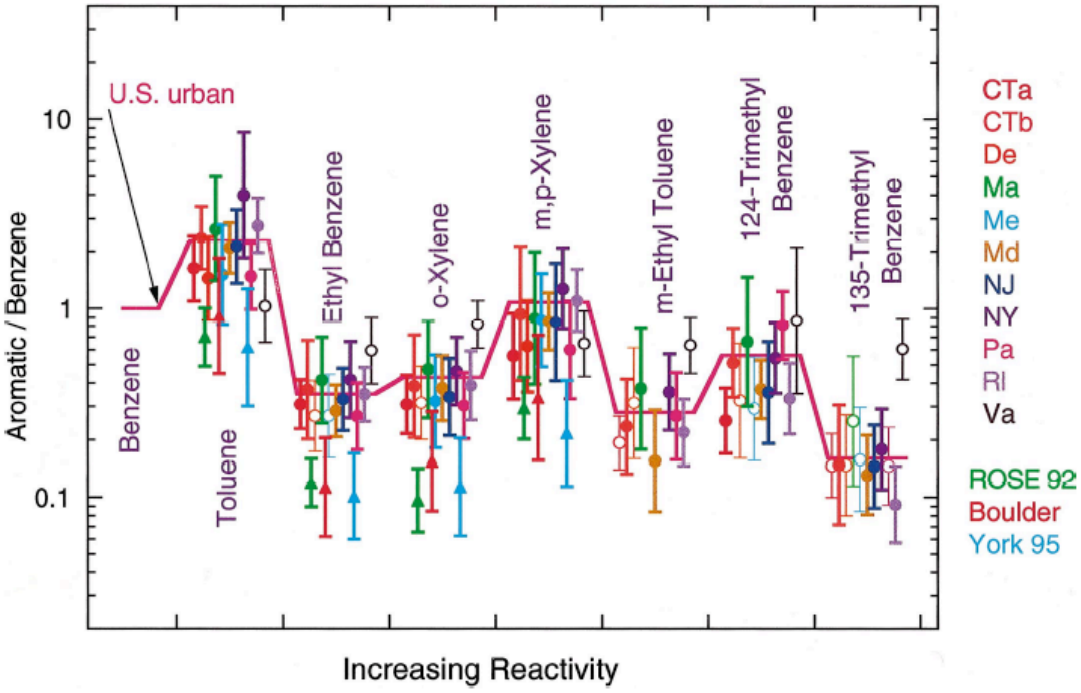
U.S. urban
Benzene
Toluene
Ethyl Benzene
o-Xylene
m,p-Xylene
m-Ethyl Toluene
124-Trimethyl Benzene
135-Trimethyl Benzene
Aromatic / Benzene
10
1
0.1
Increasing Reactivity
CTa
CTb
De
Ma
Me
Md
NJ
NY
Pa
RI
Va
ROSE 92
Boulder
York 95

(a)

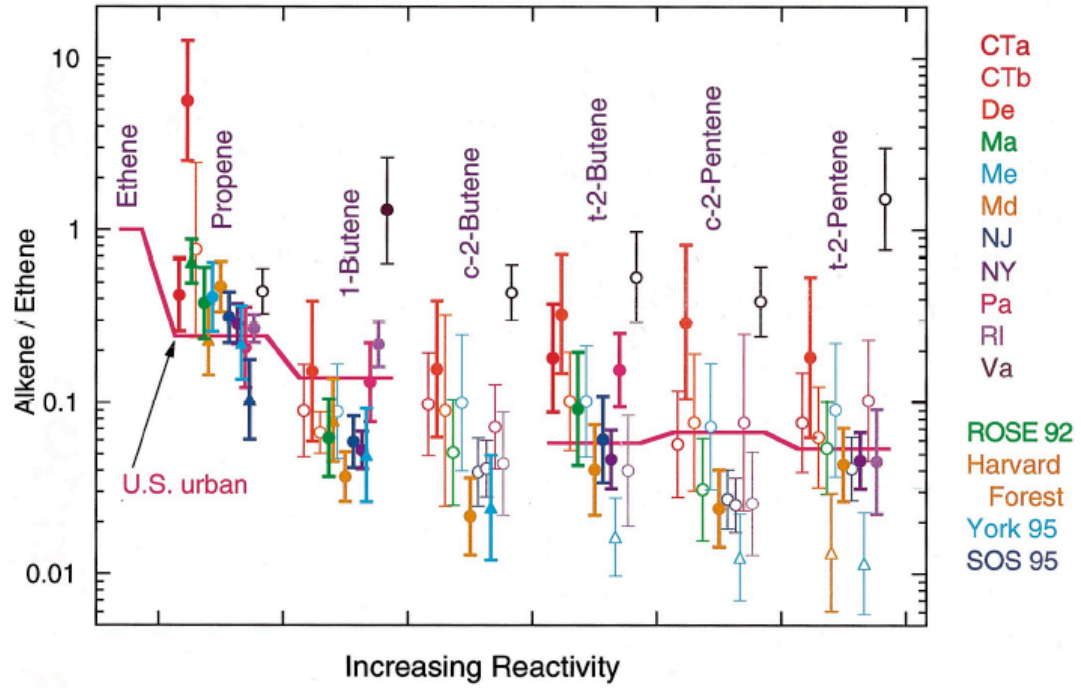
Ethene
Propene
1-Butene
c-2-Butene
t-2-Butene
c-2-Pentene
t-2-Pentene
U.S. urban
Alkene / Ethene
10
1
0.1
0.01
Increasing Reactivity
CTa
CTb
De
Ma
Me
Md
NJ
NY
Pa
RI
Va
ROSE 92
Harvard Forest
York 95
SOS 95

(b)

Figure 4.2. Log plots of ratios of (a) individual aromatics to benzene, and (b) individual alkenes to ethene, arranged in order of increasing reactivity or the aromatic or alkene. Each symbol and error bar gives the geometric mean and standard deviation of the labeled ratio and colored data set. The color key is on the right. PAMS and research data sets are represented by circles and triangles respectively. The symbol is closed only if more than 50% of both hydrocarbons in the ratio are above the detection limit. The solid line gives urban median ratios. From Parrish et al. (2000).

==========

4.3. Practical implementation.

The following steps are proposed as a basis for evaluating ozone formation in an urban area based on a data set with measured VOC and either NO_x or NO_y. The evaluation should include four major components:

1. Evaluation of measured VOC for consistency, based Parrish et al. (1998, 2000). *Recommended method*: Plot the ratio of individual species relative to a reference hydrocarbon for each of the major reaction classes (alkanes, alkenes, aromatics), on comparison with standard ratios reported by Parrish et al., or with ratios from emission inventories for the specific metropolitan area.

2. Evaluation of measured VOC and NO_x for comparison with emission inventories. *Recommended method*: Plot correlations of each VOC surrogate or reaction class versus a reference (e.g. alkanes) from the data set and from chemistry/transport models. Similarly, plot NO_x or NO_y versus a reference hydrocarbon class, and compare with the equivalent plot from chemistry/transport models.

3. Evaluation of isoprene. *Recommended method*: Plot the measured diurnal profile of isoprene in comparison with chemistry/transport model results. WARNING: Model-measurement discrepancies for isoprene (especially during the early morning or late afternoon) may be due to the rate of daytime vertical mixing in the chemistry/transport model. Isoprene in the model should show a vertical profile during midday that is comparable to previously measured vertical profiles (see **Figure 4.3**).

4. Evaluation for NO_x-VOC sensitivity. *Recommended method*: Plot reactivity-weighted VOC versus NO_x (or NO_y)for all measurement sites in the metropolitan area, in comparison with results from photochemical models for the same locations. It may be useful to do this separately for measurements during the morning (which relate most closely to emission rates for anthropogenic species) and during midday and afternoon (which relate to photochemical formation).

This representation forms a surrogate evaluation for NO_x-VOC sensitivity because the sensitivity of ozone production rates is related to NO_x-VOC sensitivity. A consistent bias towards underprediction or overprediction would suggest that the model application may be biased in its NO_x-VOC predictions.

Plots of rVOC versus NO_x or NO_y are advantageous because they can easily be used to evaluate chemistry/transport models. A consistent bias towards underprediction or overprediction would suggest that the model application may be biased in its NO_x-VOC predictions. (**Criteria** are needed to evaluate model performance.)

Methods recommended by Kleinman et al. or Cardelino et al., discussed above, are equally valid alternatives for evaluating NO_x-VOC sensitivity based on measured NO_x and VOC.

Modifications based on measurement results: The evaluation of emission inventories may suggest a systematic underestimate or overestimate of one class of VOC, or of NO_x. This might be used to generate an alternative model scenario with adjusted emission rates that would show better agreement with measurements. Mendoza-Dominguez and Russell (2000, 2001) have formalized this using inverse modeling.

If either NO_y or HNO_3 is available, the modified model scenario can be evaluated using indicator correlations (see Section 2). Results that show both improved agreement with both primary VOC and NO_x and also better agreement with the secondary indicator correlations (O_3 vs. NO_y, O_3 vs HNO_3, etc.) would suggest that the alternative scenario is more accurate.

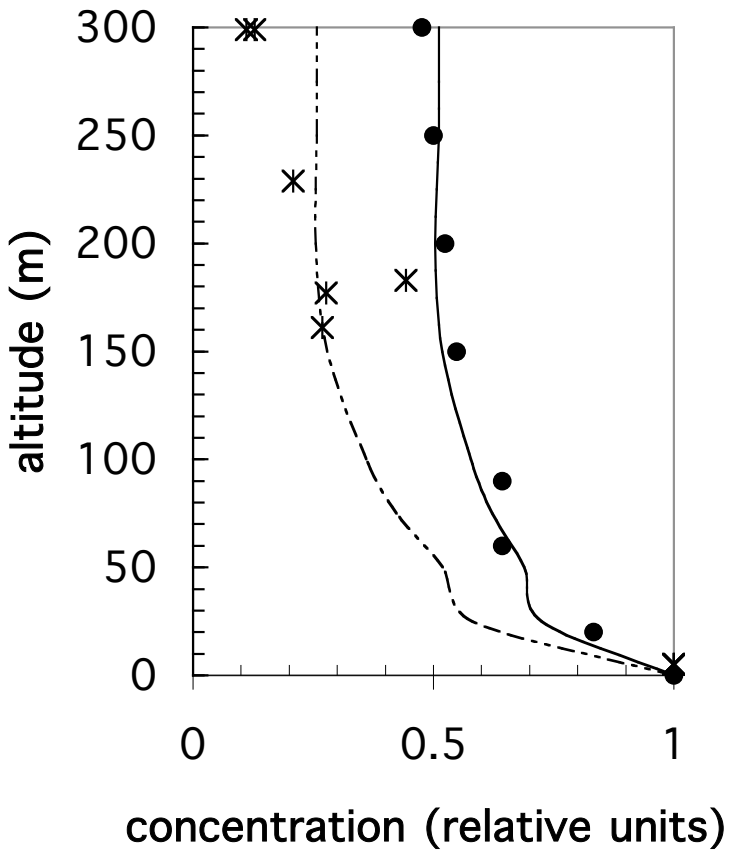

Figure 4.3. Isoprene versus altitude in meters. Isoprene is shown in units relative to surface concentrations. The solid dots represent the median profile from measurements at midday at Rose, AL (Andronache et al., 1994). The asterisks are measurements at Pellston, MI (Sillman et al., 2002). The solid and dashed lines represent model values.

==========

5. REFERENCES

Andronache, C., W. L. Chameides, M. O. Rodgers, J. E. Martinez, P. Zimmerman, and J. Greenberg. Vertical distribution of isoprene in the lower boundary layer of the rural and urban southern United States. *J. Geophys. Res.*, 99,16989-17000, 1994.

Blanchard, C. L., and T. Stoeckenius, Ozone response to precursor controls: comparison of data analysis methods with the predictions of photochemical air quality simulation models. *Atmos. Environ.*, 35, 1203-1216, 2001.

Blanchard, C. L., Ozone process insights from field experiments- Part III: Extent of reaction and ozone formation. Atmos. Environ. 2000, 34: 2035-2043.

Blanchard, C. L., F. W. Lurmann, P. M. Roth, H. E. Jeffries, and M. Korc, The use of ambient data to corroborate analyses of ozone control strategies, *Atmos. Environ.*, 33, 369-381, 1999.

Buhr, M., D Parrish, J. Elliot, J. Holloway, J. Carpenter, P. Goldan, W. Kuster, M. Trainer, S. Montzka, S. McKeen, and F. C. Fehsenfeld, Evaluation of ozone precursor source types using principal component analysis of ambient air measurements in rural Alabama. *J. Geophys. Res.*, 100, 22853-22860, 1995.

Buhr, M. P., M. Trainer, D. D. Parrish, R. E. Sievers, and F. C. Fehsenfeld, Assessment of pollutant emission inventories by principal component analysis of ambient air measurements, *Geophys. Res. Letters*, 19, 1009-1012, 1992.

Cardelino, C. and W. L. Chameides. An observation-based model for analyzing ozone-precursor relationships in the urban atmosphere. *J. Air Waste Manage. Assoc.*, 45, 161-180, 1995.

Cardelino, C. A. and W. L. Chameides, The application of data from photochemical assessment monitoring stations to the observation-based model, Atmos. Environ., 34, 2325-2332, 2000.

Chameides, W. L., F. Fehsenfeld, M. O. Rodgers, C. Cardellino, J. Martinez, D. Parrish, W. Lonneman, D. R. Lawson, R. A. Rasmussen, P. Zimmerman, J. Greenberg, P. Middleton, and T. Wang, Ozone precursor relationships in the ambient atmosphere. *J. Geophys. Res.*, 97, 6037-6056, 1992.

Chock, D. P., T. Y. Chang, S. L. Winkler, and B. I. Nance, The impact of an 8 h ozone air quality standard on ROG and NOx controls in Southern California. Atmos. Environ., 33, 2471-2486, 1999.

Gao, D., W. R. Stockwell and J. B. Milford, Global uncertainty analysis of a regional-scale gas phase chemical mechanism. *J. Geophys. Res.*, 101 9071-9078, 1996.

Gillani, N. V. and J. E. Pleim. Sub-grid-scale features of anthropogenic emissions of NO_X and VOC in the context of regional Eulerian models. *Atmos. Environ.*, 30, 2043-2059, 1996.

Goldan, P. D., M. Trainer, W. C. Kuster, D. D. Parrish, J. Carpenter, J. M. Roberts, J. E. Yee, and F. C. Fehsenfeld. Measurements of hydrocarbons, oxygenated hydrocarbons, carbon monoxide and nitrogen oxides in an urban basin in Colorado: implications for emissions inventories. *J. Geophys. Res.*, 100, 22771-22785, 1995.

Goldan, P. D., W. C. Kuster, and F. C. Fehsenfeld, Non-methane hydrocarbon measuremetns during the tropospheric OH photochemistry experiment, *J. Geophys. Res.*, 102, 6315-6324, 1997.

Goldan, P. D., D. D. Parrish, W. C. Kuster, M. Trainer, S. A. McKeen, J. Holloway, B. T. Jobson, D. T. Sueper, and F. C. Fehsenfeld, Airborne measurements of isoprene, CO and anthropogenic hydrocarbons and their implications, *J. Geophys. Res.*, in press, 2001.

Guenther, A., P. Zimmerman, L. Klinger, J. Greenberg, C. Ennis, K. Davis, W. Pollock, H. Westberg, G. Allwine, and C. Geron, Estimates of regional natural volatile organic compound fluxes from enclosure and ambient measurements. J. Geophys. Res., 101, 1345-1359, 1996a.

Guenther, A., W. Baugh, K. Davis, G. Hampton, P. Harley, L. Klinger, L. Vierling, P. Zimmerman, E. Allwine, S. Dilts, B. Lamb, H. Westberg, D. Baldocchi, C. Geron, and T. Pierce, Isoprene fluxes measured by enclosure, relaxed eddy accumulation, surface layer gradient, mixed layer gradient, and mixed layer mass balance techniques. J. Geophys. Res., 101, 18555-18567, 1996b.

Hammer, M.-U., B. Vogel, and H. Vogel, Findings on H_2O_2/HNO_3 as an Indicator of Ozone Sensitivity in Baden-Württemberg, Berlin-Brandenburg, and the Po Valley Based on Numerical Simulations, *J. Geophys. Res*., in press, 2001.

Henry, R. C., C. W. Lewis, P. K. Hopke, and H. W. Williamson, Review of receptor modeling fundamentals, Atmos. Environ., 18, 1507-1515, 1984.

Hirsch, A. I., J. W. Munger, D. J. Jacob, L. W. Horowitz, and A. H. Goldstein, Seasonal variation of the ozone production efficiency per unit NO_X at Harvard Forest, Massachusetts. *J. Geophys. Res*., 101, 12659-12666, 1996.

Jacob, D. J., B. G. Heikes, R. R. Dickerson, R. S. Artz and W. C. Keene. Evidence for a seasonal transition from NO_X- to hydrocarbon-limited ozone production at Shenandoah National Park, Virginia. *J. Geophys. Res*., 100, 9315-9324, 1995.

Jaegle, L., D.J. Jacob, W.H. Brune, D. Tan, I. Faloona, A.J. Weinheimer, B.A. Ridley, T.L. Campos, and G.W. Sachse, Sources of HOx and production of ozone in the upper troposphere over the United States, Geophys. Res. Lett., 25, 1705-1708, 1998.

Kim, B. M. and R. C. Henry, Application of SAFER model to tbe Los Angeles PM10 data, *Atmos. Environ.*, 34, 1747-1759, 2000.

Kirchner, F., F. Jeaneret, A. Clappier, B. Kruger, H. van den Bergh, and B. Calpini, Total VOC reactivity in the planetary boundary layer 2. A new indicator for determining the sensitivity of the ozone production to VOC and NOx, J. Geophys. Res., 106, 3095-3110, 2001.

Kleinman, L. H., P. H. Daum, Y-N. Lee, L. J. Nunnermacker, S. R. Springston, J. Weinstein-Lloyd, and Jochen Rudolph, Sensitivity of ozone production rate to ozone precursors, Geophys. Res. Lett.,28, 2903-2906, 2001, 2001.

Kleinman, L. I., P. H. Daum,Y-N. Lee, L. J. Nunnermacker, S. R. Springston, J. Weinstein-Lloyd, P. Hyde, P. Doskey, J. Rudolf, J. Fast and C. Berkowitz, Photochemical age determinations in the Phoenix metropolitan area. J. Geophys. Res., 10.1029/2002JD002621, 2003.

Kleinman, L. I., P. H. Daum, D. G. Imre, J. H. Lee, Y-N. Lee, L. J. Nunnermacker, S. R. Springston, J. Weinstein-Lloyd, and L. Newman, Ozone production in the New York City urban plume, J.Geophys. Res., 105, 14495-14511, 2000.

Kleinman, L. I., Ozone procuess insights from field experiments – part II; observation-based analysis for ozone production. Atmos. Environ., 34, 2023-2034, 2000.

Kleinman, L. I., P. H. Daum, J. H. Lee, Y-N. Lee, L. J. Nunnermacker, S. R. Springston, L. Newman, J. Weinstein-Lloyd and S. Sillman. Dependence of ozone production on NO and hydrocarbons in the troposphere. *Geophys. Res. Lett*., 24, 2299-2302, 1997.

Kleinman, L. I., Low and high-NO_X tropospheric photochemistry. *J. Geophys. Res.,* 99, 16831-16838, 1994.

Lin, X., M. Trainer, and S. C. Liu, On the nonlinearity of tropospheric ozone, *J. Geophys Res.*, 93, 15879-15888, 1988.

Liu, S. C., M. Trainer, F. C. Fehsenfeld, D. D. Parrish, E. J. Williams, D. W. Fahey, G. Hubler, ad P. C. Murphy, Ozone production in the rural troposphere and the implications for regional and global ozone distributions. J. Geophys. Res., 92, 4191-4207, 1987.

Lu, C-H. and J. S. Chang. On the indicator-based approach to assess ozone sensitivities and emissions features. J. Geophys. Res., 103, 3453-3462, 1998.

Luke, W. T., T. B. Wtson, K. J. Olszyna, R. Laureen Gunter, R. T. McMillen, D. L. Wellman, and S. W. Wilkison, Comparison of airborne and surface trace gas measurements during the Southern Oxidant Study, J. Geophys. Res., 103, 22317-22337, 1998.

Martilli, A., A. Neftel, G. Favaro, F. Kirchner, S. Sillman, and A. Clappier, Simulation of the ozone formation in the northern part of the Po Valley with the TVM-CTM. *J. Geophys. Res*., in press, 2001.

McClenny, W. A. ed, Recommended Methods for Ambient Air Monitoring of NO, NO2, NOy, and Individual NOz Species, EPA/600/R-01/005, September, 2000.

Mendoza-Dominguez, A., J. W. Boylan, Y-J. Yang and A. G. Russell, Efficient sensitivity analysis of an air quality model for primary and secondary aerosol source impact quantification, submitted to J. Geophys. Res., 2002.

Mendoza-Dominguez, A., and A. G. Russell, Estimation of emission adjustments from the application of four-dimensional data assimilation to photochemical air quality modeling, Atmospheric Environment, 35, 2879-2894, 2001.

Mendoza-Dominguez and Russell, Iterative Inverse Modeling and Direct Sensitivity Analysis of a Photochemical Air Quality Model, Environ. Sci. Technol., 3, 4974-4981, 2000.

Milford, J., D. Gao, S. Sillman, P. Blossey, and A. G. Russell. Total reactive nitrogen (NO_Y) as an indicator for the sensitivity of ozone to NO_X and hydrocarbons. *J. Geophys. Res.* , 99, 3533-3542, 1994.

Milford, J., A. G. Russell, and G. J. McRae, A new approach to photochemical pollution control: implications of spatial patterns in pollutant responses to reductions in nitrogen oxides and reactive organic gas emissions. *Environ. Sci. Tech.* **23**, 1290-1301, 1989.

NARSTO. An Assessment of Tropospheric Ozone Pollution: A North American Perspective. The NARSTO Synthesis Team, July, 2000.

Parrish, D. D., et al., Internal consistency tests for evaluation of measurements of anthropogenic hydrocarbons in the troposphere, *J. Geophys. Res.*,, 103, 22,339-22,359, 1998.

Parrish, D.D., and F.C. Fehsenfeld, Methods for gas-phase measurements of ozone, ozone precursors and aerosol precursors, *Atmos, Environ.*, 34, 1921-1957, 2000.

Pierce, T., C. Geron, L. Bender, R. Dennis, G. Tonnesen, and A. Guenther, Influence of increased isopreneemissions on regional ozone modeling, J. Geophys. Res.,103, 25611-25630, 1998.

Reynolds, S., H. Michaels, P. Roth, T. W. Tesche, D. McNally, L. Gardner, and G. Yarwood, Alternative base cases in photochemical modeling: their construction, role, and value. *Atmos. Environ.*, 30, 12, 1977-1988, 1996.

Sillman, S. The use of NO_y, H_2O_2 and HNO_3 as indicators for O_3-NO_x-ROG sensitivity in urban locations. *J. Geophys. Res.*, 100, 14175-14188, 1995.

Sillman, S., K. Al-Wali, F. J. Marsik, P. Nowatski, P. J. Samson, M. O. Rodgers, L. J. Garland, J. E. Martinez, C. Stoneking, R. E. Imhoff, J-H. Lee, J. B. Weinstein-Lloyd, L. Newman and V. Aneja. Photochemistry of ozone formation in Atlanta, GA: models and measurements. *Atmos. Environ.*, 29, 3055-3066, 1995.

Sillman, S., D. He, C. Cardelino and R. E. Imhoff. The use of photochemical indicators to evaluate ozone-NO_x-hydrocarbon sensitivity: Case studies from Atlanta, New York and Los Angeles. *J. Air Waste Manage. Assoc.*, 47, 642-652, September, 1997.

Sillman, S., D. He, M. Pippin, P. Daum, L. Kleinman, J. H. Lee and J. Weinstein-Lloyd. Model correlations for ozone, reactive nitrogen and peroxides for Nashville in comparison with measurements: implications for VOC-NOx sensitivity. *J. Geophys. Res.* 103, 22629-22644, 1998.

Sillman, S., M. T. Odman, and A. G. Russell, Comment on "On the indicator-based approach to assess ozone sensitivities and emissions features" by C-H. Lu and J. S. Chang, *J. Geophys. Res.*, 106 , D18 , 20,941, 2001.

Sillman, S., Comment on 'The Impact of An 8-hour Ozone Air Quality Standard on VOC and NOx Controls in Southern California' by Chock, et al., Atmos. Environ. 35, 3370-3371, 2001.

Sillman, S., and D. He, Some theoretical results concerning O_3-NO_x-VOC chemistry and NO_x-VOC indicators, *J. Geophys. Res.*, 107, D22, 4659, doi:10.1029/2001JD001123, 2002.

Sillman, S., Carroll, M. A., Thornberry, T., Lamb, B. K., Westberg, H., Brune, W. H., Faloona, I., Tan, D., Hurst, J. M., Shepson, P. B., Sumner, A., Hastie, D. R., Mihele, C. M., Apel, E. C., Riemer, D. D., and Zika, R. G. Loss of isoprene and sources of nighttime OH radicals at a rural site in the U.S.: Results from photochemical models. J. Geophys. Res. , 107 (D5), 10.1029/2001JD000449, 2002.

Sillman, S., R. Vautard, L. Menut, and D. Kley, O_3-NO_x-VOC sensitivity and NO_x-VOC indicators in Paris: results from models and ESQUIF measurements, *J. Geophys. Res.*, in press, 2003.

Sosa, G., J. West, F. San Martini, L. T. Molina and M. J. Molina, "Air Quality Modeling and Data Analysis for Ozone and Particulates in Mexico City." MIT Integrated Program on Urban, Regional and Global Air Pollution Report No. 15, 76 pages, October 2000, available from http://eaps.mit.edu/megacities/index.html.

Thielman, A., A. S. H. Prevot, and J. Staelhelin, Sensitivity of ozone production derived from field measurements in the Italian Po Basin, *J. Geophys. Res.*, in press, 2001b.

Tonnesen, G. S. and R. L. Dennis, Analysis of radical propagation efficiency to assess ozone sensitivity to hydrocarbons and NO_x. Part 1: Local indicators of odd oxygen production sensitivity, J. Geophys. Res., 105, 9213-9225, 2000a.

Tonnesen, G. S., and R. L. Dennis, Analysis of radical propagation efficiency to assess ozone sensitivity to hydrocarbons and NO_x. Part 2:Long-lived species as indicators of ozone concentration sensitivity, J. Geophys. Res., 105, 9227-9241, 2000b.

Trainer, M., D. d. Parrish, P. d. Golday, J. Roberts, and F. C. Fehsenfeld, Review of observation-based analysis of the regional factors influencing ozone concentrations, Atmos. Environ., 34, 2045-2061, 2000.

Trainer, M., D. D. Parrish, M. P. Buhr, R. B. Norton, F. C. Fehsenfeld, K. G. Anlauf, J. W. Bottenheim, Y.Z. Tang, H.A. Wiebe, J.M. Roberts, R.L. Tanner, L. Newman, V.C. Bowersox, J.M. Maugher, K.J. Olszyna, M.O. Rodgers, T. Wang, H. Berresheim, and K. Demerjian. Correlation of ozone with NO_y in photochemically aged air. *J. Geophys. Res.*, 98, 2917-2926, 1993.

Vogel, B., N., Riemer, H. Vogel, F. Fiedler, Findings on NOy as an indicator for ozone sensitivity based on different numerical simulations, *J. Geophys. Res.*, 3605-3620, 1999.

Watson, J. G., J. C. Chow, and E. M. Fujita, Review of volatile organic compound source apportionment by chemical mass balance, *Atmos. Environ.*, 35, 1567-1584, 2001.

==========